

# Discovery of the First *N*-Hydroxycinnamamide-Based Histone Deacetylase 1/3 Dual Inhibitors with Potent Oral Antitumor Activity

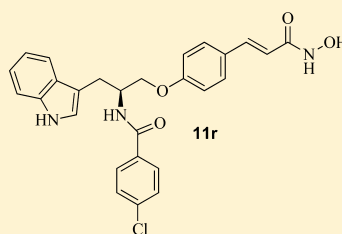
Xiaoyang Li,<sup>†</sup> Elizabeth S. Inks,<sup>‡</sup> Xiaoguang Li,<sup>†</sup> Jinning Hou,<sup>†</sup> C. James Chou,<sup>‡</sup> Jian Zhang,<sup>†</sup> Yuqi Jiang,<sup>†</sup> Yingjie Zhang,<sup>\*†</sup> and Wenfang Xu<sup>\*†</sup>

<sup>†</sup>Department of Medicinal Chemistry, School of Pharmacy, Shandong University, Ji'nan, Shandong 250012, P. R. China

<sup>‡</sup>Department of Drug Discovery and Biomedical Sciences, South Carolina College of Pharmacy, Medical University of South Carolina, Charleston, South Carolina 29425, United States

## S Supporting Information

**ABSTRACT:** In our previous study, we designed and synthesized a novel series of *N*-hydroxycinnamamide-based HDAC inhibitors (HDACIs), among which the representative compound **14a** exhibited promising HDACs inhibition and antitumor activity. In this current study, we report the development of a more potent class of *N*-hydroxycinnamamide-based HDACIs, using **14a** as lead, among which, compound **11r** gave IC<sub>50</sub> values of 11.8, 498.1, 3.9, 2000.8, 5700.4, 308.2, and 900.4 nM for the inhibition of HDAC1, HDAC2, HDAC3, HDAC4, HDAC6, and HDAC11, exhibiting dual HDAC1/3 selectivity. Compounds **11e**, **11r**, **11w**, and **11y** showed excellent growth inhibition in multiple tumor cell lines. In vivo antitumor assay in U937 xenograft model identified compound **11r** as a potent, orally active HDACI. To the best of our knowledge, this work constitutes the first report of oral active *N*-hydroxycinnamamide-based HDACIs with dual HDAC1/3 selectivity.



Class I	HDAC1 IC <sub>50</sub>	11.8 nM
	HDAC2 IC <sub>50</sub>	498.1 nM
	HDAC3 IC <sub>50</sub>	3.9 nM
	HDAC8 IC <sub>50</sub>	2000.8 nM
Class II a	HDAC4 IC <sub>50</sub>	5700.7 nM
Class II b	HDAC6 IC <sub>50</sub>	308.2 nM
Class IV	HDAC11 IC <sub>50</sub>	900.4 nM

HDAC1, HDAC2, HDAC3, HDAC4, HDAC6, and HDAC11, exhibiting dual HDAC1/3 selectivity. Compounds **11e**, **11r**, **11w**, and **11y** showed excellent growth inhibition in multiple tumor cell lines. In vivo antitumor assay in U937 xenograft model identified compound **11r** as a potent, orally active HDACI. To the best of our knowledge, this work constitutes the first report of oral active *N*-hydroxycinnamamide-based HDACIs with dual HDAC1/3 selectivity.

## INTRODUCTION

Epigenetics are widely implicated in tumor initiation and progression by different modifications of DNA and histones. There is a growing body of evidence demonstrating the importance of histone modification in silencing tumor suppressor genes.<sup>1</sup> Among the various histone modifiers, histone acetyltransferases (HATs) and histone deacetylases (HDACs) are two reversible enzymes regulating histone acetylation status, attaching or removing acetyl groups from the lysine residues in histone tails.<sup>2</sup> HATs prevent the positive lysine residues from interacting more closely with the DNA phosphate backbone, resulting in an "open" chromatin state, whereas the HDACs remove acetyl groups, resulting in a "closed" configuration, which blocks the access of the transcription machinery to DNA, suppressing gene expression.<sup>3</sup>

To date, 18 mammalian HDAC isoforms have been identified in humans; 11 of them (Class I, II, IV) are Zn<sup>2+</sup>-dependent HDAC enzymes (classical HDACs).<sup>4</sup> Class I HDAC, comprising HDAC 1, 2, 3, and 8, are homologous to yeast *RPD3* (reduced potassium dependency-3) protein; class II members include HDAC 4, 5, 6, 7, 9, and 10 and are structurally related to yeast *Hda 1* (histone deacetylases 1). Class IV HDAC has the sole member, HDAC11. Class III HDACs, called Sirtuins (SIRT1–7), require NAD<sup>+</sup> for their activity.<sup>5</sup>

HDAC1 mainly localizes in the nucleus due to lack of the nucleus export signal. The knockout of HDAC1 in mice caused proliferation defects and development retardation because of an arrest of cell growth that is associated with upregulation of the

p21 and p27 (cyclin-dependent Kinase inhibitors).<sup>6</sup> A recent study showed that HDAC1 largely accumulated in mature areas of differentiated tumor on the mice with teratoma, indicating that HDAC1 is a possible biomarker of benign teratoma.<sup>7</sup> HDAC3 is one of the most frequently upregulated genes in human cancers<sup>8</sup> and is involved in each of the three major targets of cancer therapy: cell cycle control, differentiation, and apoptosis.<sup>9</sup> There are many direct links between HDAC3 and various tumor types. In colon cancer cells HCT116 and Caco-2, silencing of HDAC3 expression resulted in growth inhibition, a decrease in cell survival, and increased apoptosis through stimulating p21 promoter activity and expression.<sup>10</sup> In HeLa cells, the majority of cellular HDAC3 is found to associate with SMRT and N-CoR complexes, and knockdown of HDAC3 resulted in hyperacetylation of histone H3 and apoptosis.<sup>9,11</sup> In metastatic breast cancer cell MDA-MB-231, HDAC3 efficiently inhibited CREB3-enhanced NF-κB activation. Moreover, high HDAC3 expression is also associated with gastric cancer,<sup>12</sup> Glioma,<sup>13</sup> renal cancer,<sup>14</sup> liver cancer,<sup>15</sup> and chronic lymphocytic leukemia.<sup>16</sup> On the basis of the above evidence, developing HDACIs more specifically against HDAC1/3 may prove to be a worthwhile goal.

In the past 10 years, over 490 clinical trials of more than 20 HDACIs candidates have been initiated, culminating in the approval of two antitumor drugs vorinostat (SAHA) and romidepsin (FK228). Recently, development of class or isoform

Received: December 5, 2013

Published: April 2, 2014



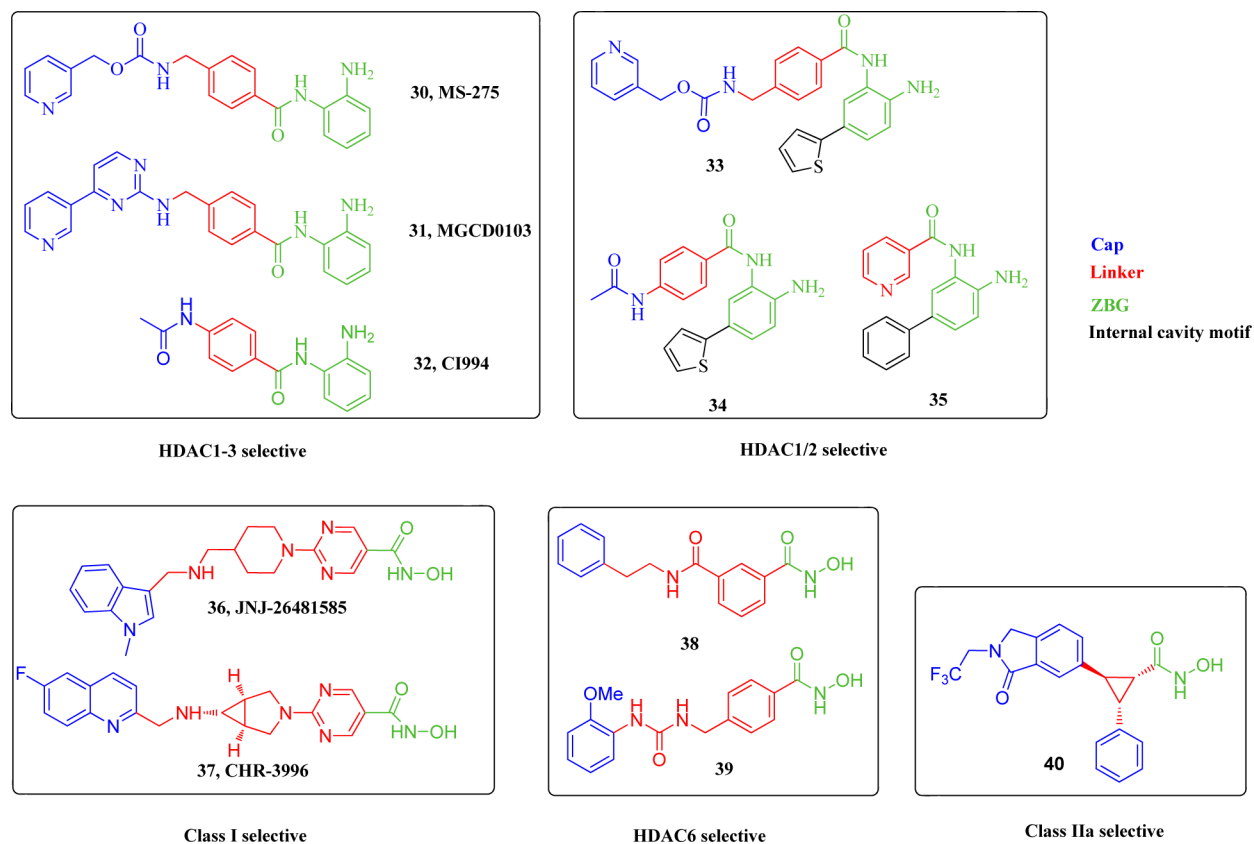


**Figure 1.** Structure of selective HDACIs.

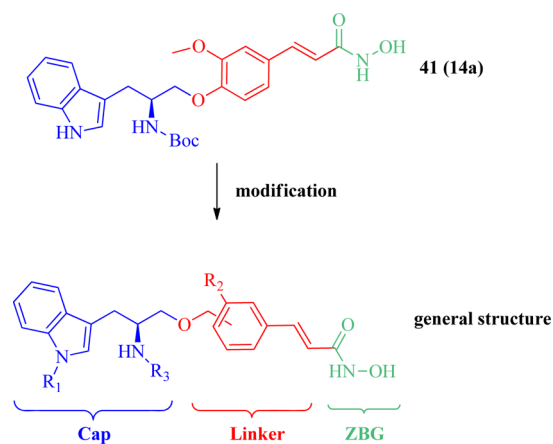
selective HDACIs has drawn increased attention. Although selective HDACIs were hypothesized to have fewer side effects than other pan-HDACIs, their therapeutic advantages have yet to be confirmed clinically. HDACIs are classified into different classes depending on their chemical structures, namely, hydroxamates, benzamides, aliphatic acids, cyclic tetra peptides, electrophilic ketones, and miscellaneous groups, among which hydroxamates are considered as the most common HDACIs. Although some class I selective,<sup>17,18</sup> HDAC6 (class IIb)<sup>19</sup> selective, and class IIa<sup>20</sup> selective hydroxamate inhibitors have been reported (Figure 1), hydroxamates are generally thought to have limitation in selectivity against desired HDAC isoforms due to their very strong chelating ability with zinc ion.<sup>21</sup> To the best of our knowledge, most of the subclass I selective inhibitors in research are benzamide HDACIs, such as MS-275 (30), MGCD0103 (31), CI994 (32), and so on (Figure 1).<sup>22,23</sup> Additionally, recent study demonstrated aryl substituents in the *o*-phenylenediamine of benzamide HDACIs led to dramatic improvements in potency and selectivity for HDAC1 and 2 versus HDAC3 (Figure 1).<sup>24,25</sup>

Recently, we have embarked on development of *N*-hydroxycinnamide-based HDACIs; in our previous study, compound (*S,E*)-*tert*-butyl (1-(4-(3-(hydroxyamino)-3-oxoprop-1-en-1-yl)-2-methoxyphenoxy)-3-(1*H*-indol-3-yl)propan-2-yl)carbamate (14a) exhibited modest HDAC inhibitory.<sup>26</sup> Here in this article, we report the design, synthesis, and biological evaluation of a new series of selective hydroxamate HDACIs describing their structure–activity relationship (SAR) studies, isotype-selectivity, and anticancer activities. The representative compound 11r shows dual selectivity and high potency toward HDAC1/3. Several compounds show an excellent effect in proliferation inhibition against U937, HEL,

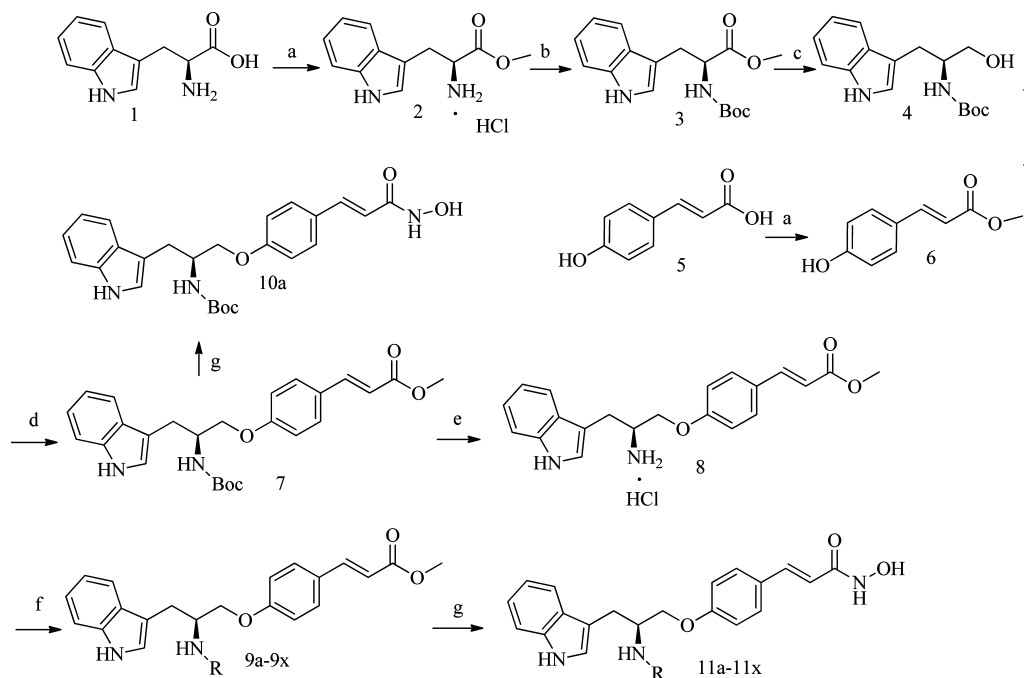
KG1, HL60, K562, PC-3, A549, MDA-MB-231, HCT116, and MCF-7 cell lines. In vivo antitumor assay in U937 xenograft model showed compound 11r is a potent, orally active HDACI.

## RESULTS AND DISCUSSION

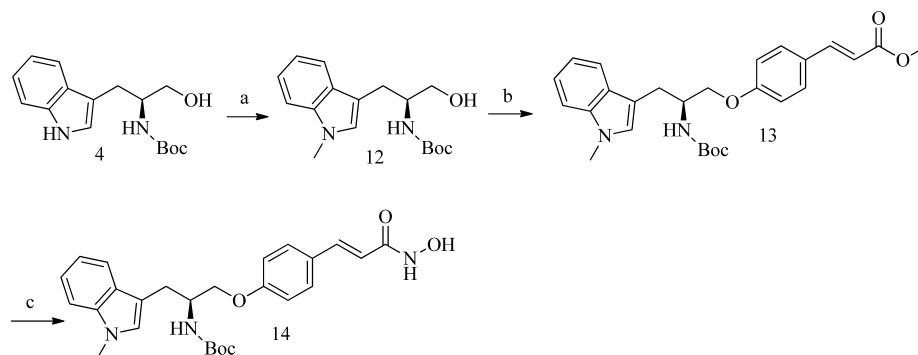
**Chemistry.** We designed and synthesized a library of cinnamamide derivatives based on the lead compound 41 (14a) (Figure 2). The library was designed to fully explore the influence of variation in the methoxy group of ferulic acid and the cap group. The synthesis of compounds 10a and its derivatives 11a–11x is described in Scheme 1. Synthesis of 3 was started with *L*-try by methyl ester protection and Boc-protection. Methyl ester protection of 4-hydroxycinnamic acid



**Figure 2.** Modification site and general structure of target compounds.

Scheme 1. Synthesis of Compounds 10a–11y<sup>a</sup>

<sup>a</sup>Reagents and conditions: (a)  $\text{CH}_3\text{COCl}$ ,  $\text{CH}_3\text{OH}$ , 95%; (b)  $(\text{Boc})_2\text{O}$ ,  $\text{Et}_3\text{N}$ ,  $\text{CH}_2\text{Cl}_2$ , 90%; (c)  $\text{LiAlH}_4$ , anhydrous THF, 86%; (d)  $\text{PPh}_3$ , DEAD, anhydrous THF, 55%; (e)  $\text{AcOEt}/\text{HCl}$ , 80%; (f) carboxylic acids or Boc-protected amino acids, TBTU,  $\text{Et}_3\text{N}$ , anhydrous  $\text{CH}_2\text{Cl}_2$  (60–65%); (g)  $\text{NH}_2\text{OH}$ ,  $\text{KOH}$ , anhydrous  $\text{CH}_3\text{OH}$ , (30–40%).

Scheme 2. Synthesis of Compound 14<sup>a</sup>

<sup>a</sup>Reagents and conditions: (a)  $\text{CH}_3\text{I}$ ,  $\text{KOH}$ , TBABr,  $\text{H}_2\text{O}$ , THF, 50%; (b)  $\text{PPh}_3$ , DEAD, anhydrous THF, 55%; (c)  $\text{NH}_2\text{OK}$ , anhydrous  $\text{CH}_3\text{OH}$ , 30%.

5 gave 6. Reduction of 3 by  $\text{LiAlH}_4$  led to 4, which was further subjected to Mitsunobu reaction with 6 and gave 7. Compound 7 was directly converted to the target hydroxamic acid 10a. Intermediate 8, the *N*-deprotected product of 7, reacted with different carboxylic acids or Boc-protected amino acids by TBTU-mediated amide formation to afford 9b–9z. Compounds 9b–9z were converted to hydroxamic acid compounds 11a–11z by  $\text{NH}_2\text{OK}$  in dry methanol.

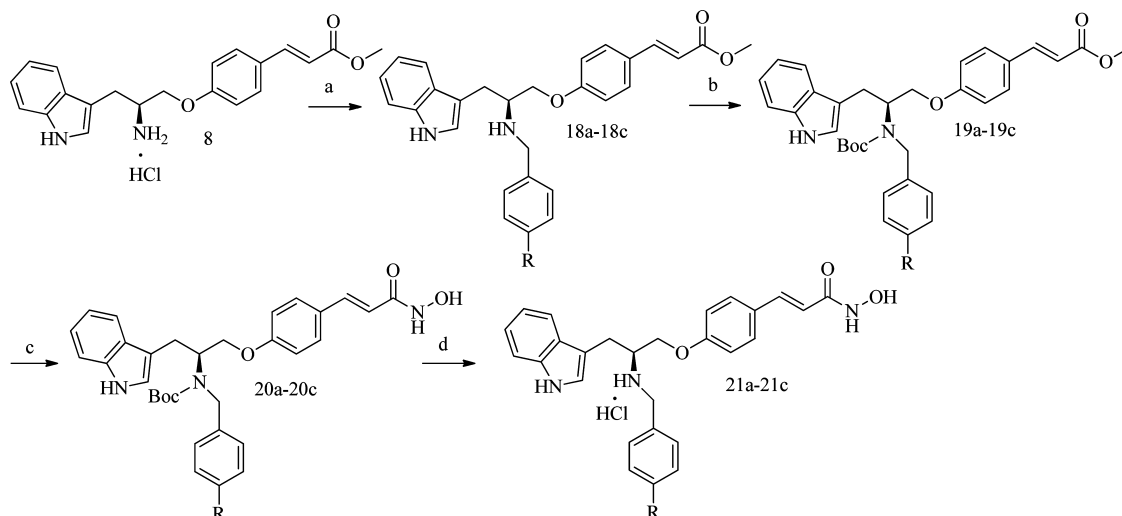
Compound 4 was treated with  $\text{CH}_3\text{I}$  and phase transfer catalyst TBABr in  $\text{H}_2\text{O}/\text{THF}$  containing  $\text{KOH}$  to get the methyl protected 12 (Scheme 2). Subsequent reaction of 12 with 6 through Mitsunobu reaction in the presence of  $\text{PPh}_3$  and DEAD afforded compound 13. Finally, the hydroxamic acid group was achieved in usual conditions to get compound 14.

Scheme 3 shows the preparation of secondary amine 21a–21c. Intermediate 8 was mixed with benzaldehyde, 4-chlorobenzaldehyde, or 4-fluorobenzaldehyde in anhydrous

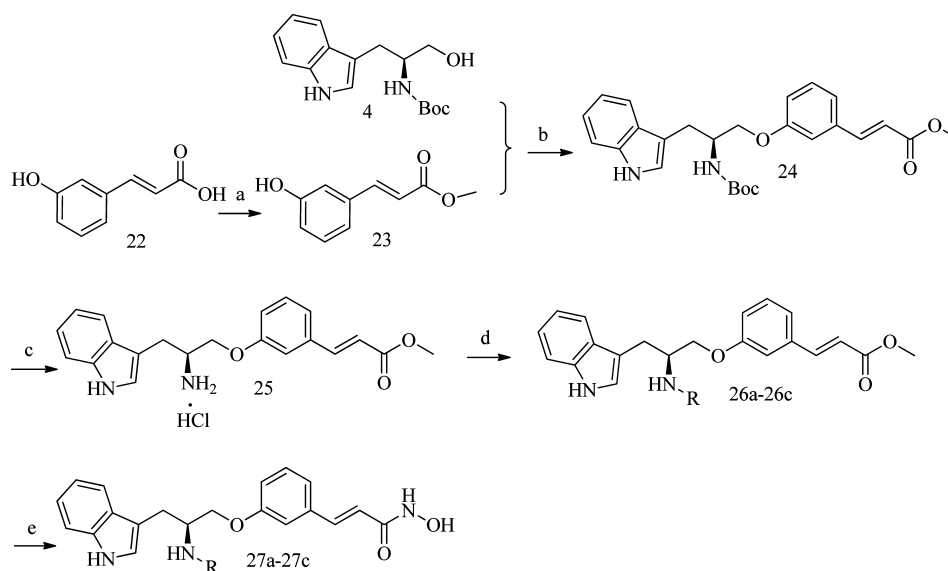
$\text{CH}_3\text{OH}$ , respectively, then  $\text{NaBH}_4$  was added to give 18a–18c. Boc-protected products 19a–19c were converted to hydroxamic acids 20a–20c. Subsequent deprotection gave the end-products 21a–21c.

Unlike Scheme 1, Scheme 4 used 3-hydroxycinnamic acid instead of 4-hydroxycinnamic acid to give another new series of compounds 27a–27c. The reagents and conditions of Scheme 4 are the same as those in Scheme 1.

**HeLa Cell Extract Inhibition of the Target Compounds.** In our previous study we found the lead compound 41 displayed modest inhibition toward HDACs.<sup>24</sup> At the beginning of our present research, we made an attempt to find a new lead compound by modifying the  $\text{R}_1$  and  $\text{R}_2$  groups of 41 (Table 1). We changed the  $\text{R}_2$  group of 41 by replacing the methoxy group with H to get compound 10a (Scheme 1) and changed the  $\text{R}_1$  group of 10a with a methyl group to get compound 14 (Scheme 2). We used HeLa cell extract as the

Scheme 3. Synthesis of Compounds 21a–21c<sup>a</sup>

<sup>a</sup>Reagents and conditions: (a) benzaldehyde (4-chlorobenzaldehyde or 4-fluorobenzaldehyde), Et<sub>3</sub>N, NaBH<sub>4</sub>, anhydrous CH<sub>3</sub>OH, 85%; (b) (Boc)<sub>2</sub>O, Et<sub>3</sub>N, CH<sub>3</sub>OH, 65%; (c) NH<sub>2</sub>OK, anhydrous CH<sub>3</sub>OH, 30–40%; (d) AcOEt/HCl, 70%.

Scheme 4. Synthesis of Compounds 27a–27c<sup>a</sup>

<sup>a</sup>Reagents and conditions: (a) CH<sub>3</sub>COCl, CH<sub>3</sub>OH, 95%; (b) PPh<sub>3</sub>, DEAD, anhydrous THF, 55%; (c) AcOEt/HCl, 80%; (d) carboxylic acids, TBTU, Et<sub>3</sub>N, anhydrous CH<sub>2</sub>Cl<sub>2</sub> (60–65%); (e) NH<sub>2</sub>OH, KOH, anhydrous CH<sub>3</sub>OH, (30–40%).

Table 1. HDAC Inhibition Activity of Compounds 41, 10a, and 13

cpd	R <sub>1</sub>	R <sub>2</sub>	IC <sub>50</sub> of HeLa extract (nM) <sup>a</sup>
41	H	CH <sub>3</sub> O	610.5 ± 20.8
10a	H	H	530.7 ± 18.6
14	CH <sub>3</sub>	H	600.1 ± 30.7

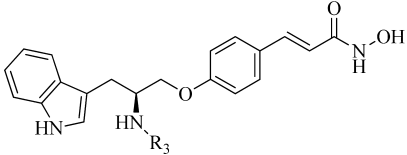
<sup>a</sup>Assays were performed in replicate ( $n \geq 2$ ); data are shown as mean ± SD.

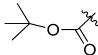
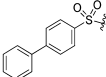
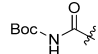
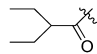
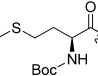
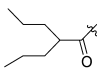
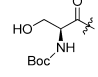
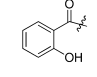
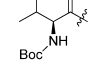
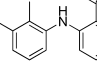
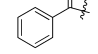
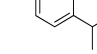
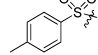
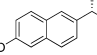
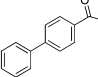
enzyme source to efficiently screen our target compounds. The result in Table 1 showed that compound 10a exhibited slightly increased HDAC inhibitory activity compared with 41 and 14. This indicated that the methoxy group in R<sub>2</sub> and methyl group in R<sub>1</sub> were not necessary, so we selected 10a as the lead compound for further optimization and modification.

In the following work, we designed an analogue to probe the effect of the *N*-substituent by replacing the Boc group of 10a with other functional groups (Scheme 1). First, we synthesized compounds 11a–11o with different substituents including Boc-protected amino acids, carboxylic acids, sulfo acids, and several anti-inflammatory acids (Table 2). It was obvious that the compounds with the structure of acid amide substituents were more potent than those with sulfamide substituents (Table 2). For example, the IC<sub>50</sub> value of 11g in HeLa extract was 1703.4 nM, much lower than compound 11h (>5000 nM). The same



Table 2. HDAC Inhibition Activity of Compounds 10a and Its Derivatives 11a–11o



Cpd	R <sub>3</sub>	IC <sub>50</sub> of Hela extract (nM) <sup>a</sup>	Cpd	R <sub>3</sub>	IC <sub>50</sub> of Hela extract (nM) <sup>a</sup>
10a		530.0 ± 18.7	11h		>5000
11a		96.6 ± 4.5	11i		130.3 ± 14.8
11b		255.1 ± 9.8	11j		977.8 ± 21.9
11c		97.6 ± 2.4	11k		20.8 ± 3.1
11d		84.3 ± 2.9	11l		673.69 ± 39.7
11e		10.5 ± 2.3	11m		1043.1 ± 89.0
11f		636.9 ± 38.7	11o		>5000
11g		1703.4 ± 137.9	SAHA		120.8 ± 5.9

<sup>a</sup>Assays were performed in replicate ( $n \geq 2$ ); data are shown as mean ± SD.

result was also shown in compounds **11e** and **11f**. Additionally, compound **11i** was more potent than **11j**, which indicated that a short side alkyl chain might advance HDAC inhibitory activity. Among compounds **11a–11o**, the most potent compounds, **11e** and **11k**, with IC<sub>50</sub> values of 15.4 and 20.8 nM, respectively, were far more potent than SAHA (120.8 nM). The common element they all share is a simple benzamide as their *N*-substituent, so further modification focused on compound **11e**.

Next, we synthesized **11p** and **11q**, which had different alkyl chain lengths relative to **11e**. Activity data showed **11e** with the shortest side chain had the best activity, which also agreed with the conclusion shown in **11i** and **11j**, that a short side alkyl chain may promote their activity. Then we synthesized compounds **11r–11y** (Scheme 1) to probe the effect of substituent in benzene ring of benzamide (Table 3). Surprisingly, the para-substituted compounds **11r**, **11w**, **11x**, and **11y** showed a marked increase in the HDAC inhibition potency compared with **11e**, the IC<sub>50</sub> values of **11r**, **11w**, **11x**, and **11y** were 5.6, 6.7, 20.4, and 4.8 nM, respectively, however, the ortho-substituted, metha-substituted, and disubstituted compounds **11s**, **11t**, **11u**, and **11v** exhibited inferior activity

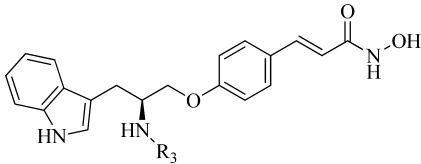
relative to **11e**. The result showed para-substituents on a benzene ring have an obvious promoting effect on HDAC inhibition.

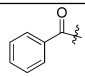
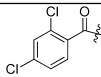
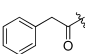
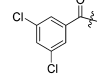
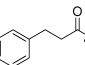
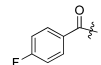
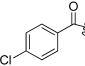
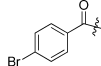
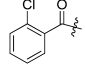
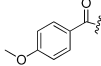
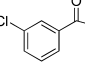
Scheme 4 was designed to evaluate the activity of 3-hydroxycinnamide-based series. We modified some of the most potent compounds, **11e**, **11r**, and **11w**, to achieve compounds **27a–27c**. The HDAC inhibition result in Table 4 showed compounds **27a–27c** exhibited poor activity compared with **11e**, **11r**, and **11w**, which revealed that 4-hydroxycinnamide-based series were superior to the 3-hydroxycinnamide-based series. Then **21a–21c** were designed to improve water solubility and chemical stability by replacing the amide of **11e**, **11r**, and **11w** with a secondary amine. Compounds **21a–21c** showed mild inhibition, and the activity was 15 times lower than **11e**, **11r**, and **11w**. The possible explanation for why compounds **11r**, **21c**, and **27c** with similar structure exhibited quite different activity was described in the molecule docking section.

#### In Vitro HDAC Isoform-Selectivity of the Compounds.

In order to explore the HDAC isoform selectivity profile, we chose the most potent compounds **11e**, **11p**, **11r**, **11w**, and **11y** described in the above discussion, as well as secondary amine

Table 3. HDAC Inhibition Activity of Compounds 11e and Its Derivatives 11p–11x



Cpd	R <sub>3</sub>	IC <sub>50</sub> of Hela extract (nM) <sup>a</sup>	Cpd	R <sub>3</sub>	IC <sub>50</sub> of Hela extract (nM) <sup>a</sup>
11e		10.5 ± 2.3	11u		186.5 ± 14.8
11p		23.2 ± 4.5	11v		209.8 ± 19.8
11q		52.3 ± 3.8	11w		6.7 ± 1.8
11r		5.6 ± 1.1	11x		20.4 ± 2.9
11s		50.4 ± 10.8	11y		4.8 ± 0.9
11t		147.9 ± 23.7			

<sup>a</sup>Assays were performed in replicate ( $n \geq 2$ ); data are shown as mean ± SD.

analogue **21c** and 3-hydroxycinnamide-based analogue **27c** to conduct enzyme inhibitory assays against HDAC1, HDAC2, HDAC3, and HDAC6. Results presented in Table 5 reveal that compounds **11e**, **11r**, **11w**, and **11y** exhibited dual selectivity against HDAC1/3, among which compound **11r** exhibited the most obvious dual selectivity, particularly against HDAC3. IC<sub>50</sub> value of **11r** against HDAC3 was 3.9 nM, which was ~80-fold and ~130-fold lower than that of HDAC6 and HDAC2, respectively. The positive control, SAHA, had almost no selectivity toward these HDAC isoforms. To ascertain the selectivities of our compounds across the broader family of HDAC isoforms, we next profiled representative **11r** against HDAC8 (class I), HDAC4 (class IIa), and HDAC11 (class IV). Compound **11r** also displayed low micromolar activity against HDAC8, HDAC4, and HDAC11 compared to the low nanomolar activity against HDAC1 and HDAC3 (Table 6). These data establish **11r** to be a potent and HDAC1/3 dual selective inhibitor.

**In Vitro Antiproliferative Assay.** Compounds **11e**, **11p**, **11r**, **11w**, and **11y** with the most potent HDACs inhibitory activity were selected to test their antiproliferative activity against 10 types of solid or hematological tumor cell lines, which were most frequently used in evaluating HDACIs (Table 7). Data showed cell lines HL60, MCF-7, and A549 had lower sensitivity with our tested compounds than the other cell lines. All the tested compounds exhibited much more superior antiproliferative potency than SAHA against U937, K562, HEL, KG1, MDA-MB-231, PC-3, and HCT116 cells. Compounds **11e**, **11r**, **11w**, and **11y**, which displayed the highest HDAC

enzyme inhibitory potency, also exhibited the best antiproliferative activity. Among these analogues, compound **11r** exhibited the highest potency, and human leukemic monocyte lymphoma U937 seemed to be the most sensitive cell line to our HDACIs. So cell line U937 was chosen for further evaluation. Furthermore, cytotoxicity of **11r** against Human Umbilical Vein Endothelial Cells (HUVEC) was tested in our lab, and the IC<sub>50</sub> value was  $61.48 \pm 6.17 \mu\text{M}$ , which revealed our compounds' selectivity over nontransformed cells when compared with tumor cells.

#### Western Blot Analysis and Flow Cytometry Analysis.

Although the HDAC inhibitory activity of our HDACIs was confirmed in cell-free assays, the results were not as clear in cell based assays. In order to investigate the HDAC inhibitory activity of our HDACIs in cells further, we chose compounds that were used in evaluating HDAC isoform-selectivity to conduct Western blot assay in U937 cell. Intracellular levels of acetylated histoneH3, acetylated histoneH4 (known substrates for HDAC1, 2, and 3), and acetylated  $\alpha$ -tubulin (a known substrate for HDAC6)<sup>27</sup> were compared with SAHA and LBH589 (one of the most potent pan-HDACIs) as reference compounds (Figure 3). Results show compounds **11e**, **11p**, **11r**, **11w**, and **11y** can markedly increase the level of acetylated histoneH3 and acetylated histoneH4, which were much superior to SAHA, while comparable to LBH589. However, the levels of acetylated  $\alpha$ -tubulin of these compounds, especially **11r**, were much lower than LBH589. These data demonstrated that some of our compounds showed lower potency against HDAC6 than class I HDACs, which is in

Table 4. HDAC Inhibition Activity of Compounds 11e, 11r, 11w, 21a–21c, and 27a–27c

Cpd	Structure	IC <sub>50</sub> of HeLa extract (nM) <sup>a</sup>	Cpd	Structure	IC <sub>50</sub> of HeLa extract (nM) <sup>a</sup>
11e		14.5 ± 1.4	21c		157.8 ± 12.1
11w		6.7 ± 1.2	27a		439.7 ± 34.8
11r		5.6 ± 2.0	27b		447.6 ± 28.9
21a		198.5 ± 12.9	27c		389.0 ± 20.8
21b		148.0 ± 15.9			

<sup>a</sup>Assays were performed in replicate ( $n \geq 2$ ); values are shown as mean ± SD.

Table 5. In Vitro Inhibition of HDACs Isoforms of Representative Compounds<sup>a</sup>

cpd	IC <sub>50</sub> of HDAC1 (nM)	IC <sub>50</sub> of HDAC2 (nM)	IC <sub>50</sub> of HDAC3 (nM)	IC <sub>50</sub> of HDAC6 (nM)	HDAC2/ HDAC3 isoform selectivity	HDAC6/ HDAC3 isoform selectivity	HDAC2/ HDAC1 isoform selectivity	HDAC6/ HDAC1 isoform selectivity
11e	10.3	535.5	14.1	142.2	37.9	10.1	51.7	13.7
11p	13.2	432.1	143.0	143.7	3.0	1.0	32.6	10.8
11r	11.8	498.1	3.9	308.2	127.7	79.0	42.2	26.1
11w	16.7	457.0	5.5	101.7	83.1	18.5	27.2	6.01
11y	6.0	413.6	3.2	185.6	129.2	58	68.7	30.8
27c	329.9	498.5	403.2	164.4	1.2	0.4	1.5	0.5
21c	355.4	791.2	47.0	293.6	16.8	6.2	2.2	0.8
SAHA	34.6	184.7	90.1	63.0	2.0	0.7	5.3	1.8

<sup>a</sup>Assays were performed in replicate ( $n \geq 2$ ); the SD values are <20% of the mean.

agreement with the isoform selectivity data observed in cell-free assays.

As our compounds displayed HDAC1/3 dual selectivity and some studies reported that knockdown of HDAC1 and HDAC3 could increase the percent of apoptotic cells in carcinoma cells,<sup>11</sup> we also evaluated the level of procaspase3 (inactive form of apoptotic effector caspase3) in U937 cells (Figure 4). Cleavage of pro-caspases3 results in the production of an active effector, caspase3, which can cleave essential structural proteins such as cytokeratins, nuclear lamins, and also

an inhibitor of caspase-activated DNase (iCAD), which liberates the DNase (CAD) to digest chromosomal DNA and cause cell death.<sup>28</sup> We can see from the result that our compounds 11e, 11k, 11r, 11w, and 11y dramatically reduced the level of procaspase3, which was most likely due to the fact that procaspase3 was cleaved to the active form (caspase3), which could promote apoptosis of U937 cells. At the same time, we performed flow cytometry analysis to confirm the effect of these compounds in inducing apoptosis. In this assay, we chose compounds 11r and 11w as representative

Table 6. In Vitro Inhibition of HDACs Isoforms of 11r<sup>a</sup>

classes of HDACs	isoforms	IC <sub>50</sub>	fold selective for HDAC3	fold selective for HDAC1
class II	HDAC1	11.8		
	HDAC2	498.1	127.7	42.2
	HDAC3	3.9		
	HDAC8	2000.8	513.0	169.6
class IIa	HDAC4	5700.7	1461.7	483.1
class IIb	HDAC6	308.2	79.0	26.1
class IV	HDAC11	900.4	230.9	76.3

<sup>a</sup>Assays were performed in replicate ( $n \geq 2$ ); the SD values are <20% of the mean.

compounds and SAHA as the positive control. Results demonstrated that 11r, 11w, and SAHA can significantly induce apoptosis in a time-dependent and dose-dependent manner. At the same concentration (1  $\mu$ M), 11r and 11w induced 61.76% and 64.25% cell apoptosis, respectively, which were much higher than that of SAHA (26.83%). Detailed activity evaluation and apoptosis mechanism studies are currently underway in our laboratory.

**Stability of Compounds in Artificial Gastric Juice, Artificial Intestinal Juice, Rat Liver Homogenate, and Human Plasma.** Having demonstrated that 11r had ideal in vitro activity, we next set out to assess its tumor growth inhibitory effects in subcutaneous cell lines and primary tumor derived xenograft models. Before we conducted the in vivo study, we developed HPLC methods to briefly study the stability of 11r in artificial gastric juice, artificial intestinal juice, rat liver homogenate, and human plasma. Compound 11r was incubated under each condition at 37 °C for 24 h, extracted, and analyzed by HPLC. We observed that 11r was stable in artificial gastric juice, artificial intestinal juice, rat liver homogenate, and human plasma (Figure 5).

**In Vivo Antitumor Activity Assay.** Because of the great stability of 11r, it was feasible to evaluate its in vivo activity orally. We established a subcutaneous U937 xenograft model using SAHA as positive control. U937 cells ( $5 \times 10^6$ ) were subcutaneously implanted in the right flanks of female nude mice (BALB/c-nu). When tumor size reached about 100 mm<sup>3</sup>, mice were randomized to five per group and were treated with compound 11r or SAHA (100 mg/kg/day) by oral gavage for 16 days. Tumor growth inhibition (TGI) and relative increment ratio (T/C) were calculated at the end of treatment to reveal the antitumor effects in tumor weight and tumor volume, respectively. Compound 11r demonstrated potent in vivo oral antitumor activity with higher TGI value (55.1%) and lower T/C value (37%) than SAHA (TGI = 32.1%; T/C =

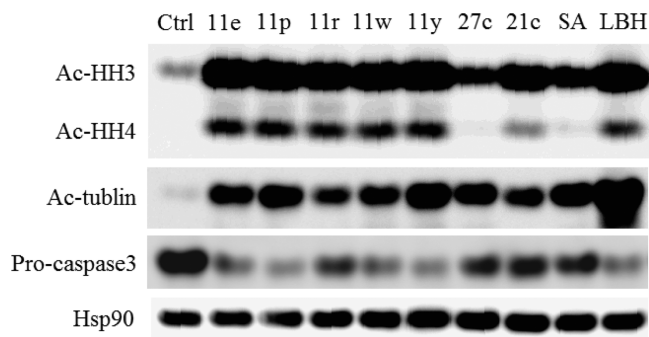


**Figure 3.** Western blot analysis of acetylated tubulin, acetylated histone H3, acetylated histone H4, and pro-caspase3 in U937 cell lines after 24 h treatment with compounds at 1  $\mu$ M using SAHA (SA) and LBH589 (LBH) as positive control. Hsp90 was used as a loading control.

47%). In the mice group treated by 11r, no significant body weight loss and no evident toxic signs in liver and spleen were detected (Figures 6 and 7).

**Docking Results.** Figure 8a revealed the docked conformation of compounds 11r, 21c, and 27c. The docked conformations of 11r and 21c were very similar in the linker and ZBG, while they were quite different in the aromatic ring and indole ring of cap group. Moreover, conformation of 27c was different from 11r and 21c, leading to diverse binding modes shown in Figure 8c–e. Figure 8c,d showed 11r and 21c had similar docking mode and hydrogen bonds; the greater potency of 11r might be amenable to the stiffening of the scaffold introduced by the amide bond, which forces the lipophilic *p*-chlorophenyl moiety to yield closer van der Waals interactions with the protein rather than projecting itself toward solvent as in 21c. Furthermore, in cap group, hydrogen bonds formed between 21c and residues Asp92 and Asp93 had a longer bond length (2.19 and 1.97 Å) than 11r (1.95 and 1.59 Å), which also might be factors that made 11r more effective against HDAC3 than 21c. Compared with 11r (Figure 8c), compound 27c (Figure 8e) could form two diverse hydrogen bonds with amide N–H of Phe200 and imidazole N–H of His172 through carbonyl oxygen atom and etheric oxygen atom, respectively, but at the same time, 27c lost two hydrogen bonds with Asp92 in the cap group and Tyr298 around zinc ion. In addition, the carbonyl oxygen of 27c had the same distance with 11r to zinc ion (2.1 Å), but the hydroxyl oxygen of 27c had a longer distance to the zinc ion (4.4 Å) than 11r (1.9 Å), which indicated that 27c could only form a weak monodentate interaction with zinc, while 11r could form a

Table 7. In Vitro Antiproliferative Activity of Representative Compounds

cpd	IC <sub>50</sub> ( $\mu$ M) <sup>a</sup>									
	U937	K562	HEL	KG1	HL60	MDA-MB-231	PC-3	MCF-7	HCT116	A549
11e	0.33	0.79	0.20	0.39	2.11	0.24	0.33	3.47	0.37	3.39
11p	0.32	0.68	0.27	0.72	1.59	0.41	0.53	2.95	0.57	3.91
11r	0.16	0.51	0.19	0.22	1.69	0.22	0.46	2.68	0.52	2.74
11w	0.18	1.01	0.19	0.24	1.04	0.27	0.51	2.7	0.37	2.96
11y	0.34	0.89	0.16	0.47	1.68	0.15	0.29	2.32	0.22	3.27
21c	0.73	0.94	0.27	0.49	2.17	0.31	0.37	3.25	0.58	3.19
SAHA	1.45	3.24	0.49	1.59	4.26	1.72	3.57	3.78	2.81	3.9

<sup>a</sup>Assays were performed in replicate ( $n \geq 2$ ); the SD values are <20% of the mean.

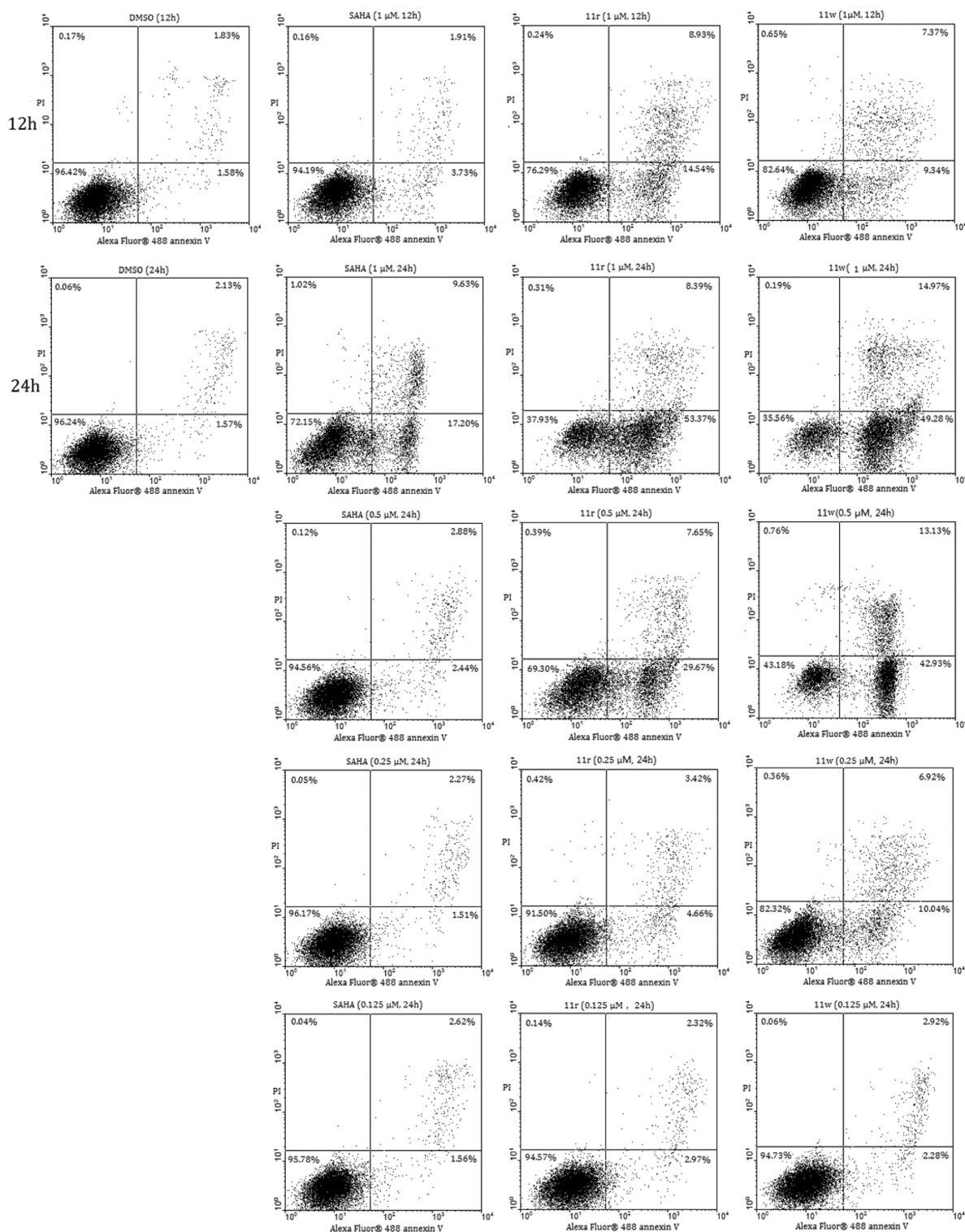


**Figure 4.** Induction of apoptosis at 12 and 24 h by compounds 11r, 11w, and SAHA in different concentrations in U937 cells.

strong bidentate interaction with zinc. This might be the reason why 27c was much less potent than 11r (Figure 8b).

## CONCLUSIONS

For the first time, *N*-hydroxycinnamide-based derivatives have been shown to be potent dual HDAC1/3 selective HDACIs. The representative compound 11r showed low nanomolar  $IC_{50}$  values against HDAC1 (11.8 nM) and HDAC3

(3.9 nM), with micromolar or submicromolar  $IC_{50}$  values against HDAC2, HDAC8, HDAC4, HDAC6, and HDAC11. In addition, a few of the examples of the new series in antiproliferative study exhibited high potency against several solid or hematological cells, even though antiproliferative activity of the compounds seemed inferior to their HDAC inhibition activity. For example, antiproliferative activity of 11r was about 10 times higher than SAHA, while its HDAC inhibition activity was about 100 times higher than SAHA. We



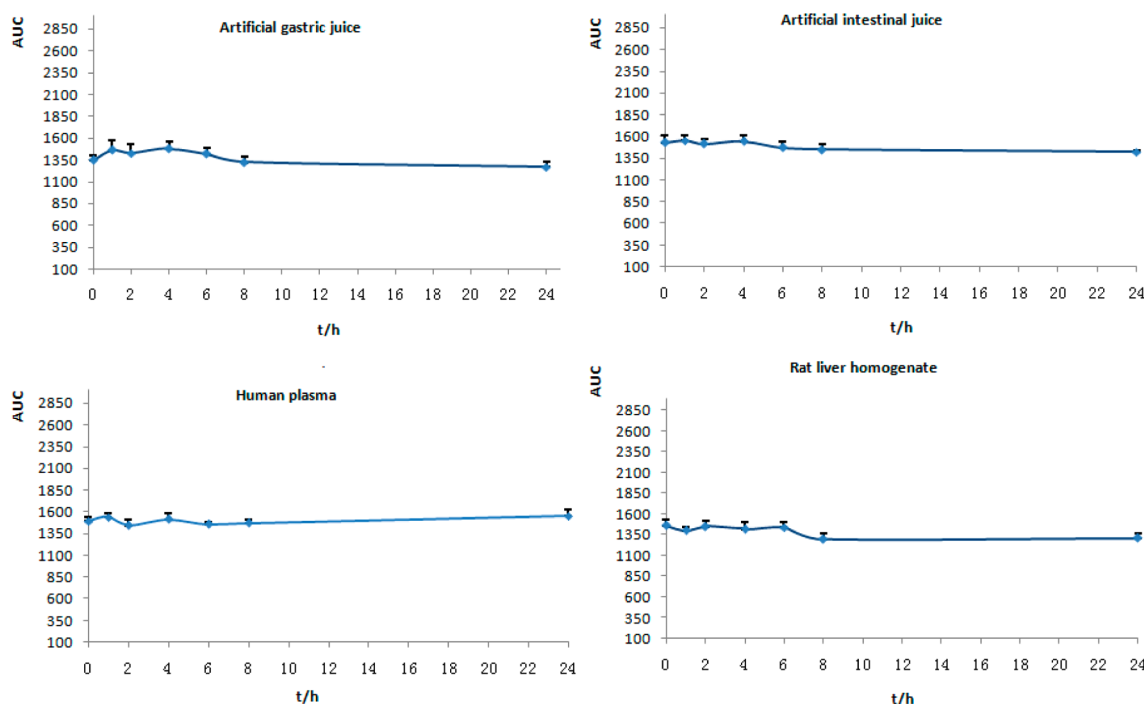


**Figure 5.** Stability of compound **11r** in artificial gastric juice, artificial intestinal juice, rat liver homogenate, and human plasma. Points were achieved after 0, 1, 2, 4, 6, 8, and 24 h, respectively, and values are shown as mean  $\pm$  SD.

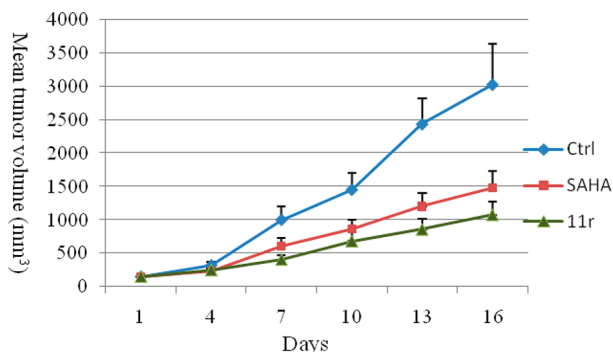


**Figure 6.** Antitumor activity comparison of **11r** and SAHA against U937 human tumor xenografts implanted in mice, expressed as mean tumor volume. Values are shown as mean  $\pm$  SD (5 mice per group).

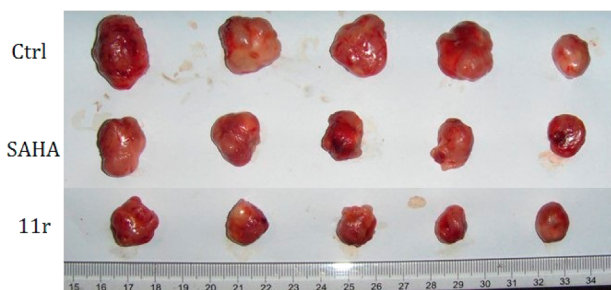


**Figure 7.** Picture of dissected U937 tumor tissues.

supposed **11r** had poor transcellular permeability; this speculation was confirmed by parallel artificial membrane permeation assay (PAMPA)<sup>29</sup> conducted on **11r** and SAHA (data not shown). Future work to improve potency should focus on enhancing permeability of **11r**.

Compound **11e**, **11r**, **11w**, and **11y** increased histone H3 and H4 acetylation in the same level of LBH589 (one of the most

potent hydroximates HDACIs in clinical) in U937 cell line. At the same time, some of the compounds decreased the level of pro-caspase3, which was consistent with the result of flow cytometry analysis in inducing apoptosis. Compound **11r** was evaluated for its in vivo antitumor study in a U937 xenograft mice model and showed higher efficacy compared to the approved drug SAHA. More detailed studies of the antitumor profiles of these promising compounds are underway in our lab. Using **11r** as lead, continued studies are underway to search for more promising HDACIs with improved transcellular permeability and isoform selectivity.

## EXPERIMENTAL SECTION

**Materials and Methods.** <sup>1</sup>H NMR spectra were obtained on a Bruker DRX spectrometer at 300 MHz with TMS as an internal standard,  $\delta$  in parts per million, and  $J$  in hertz. High-resolution mass spectrometry was performed by Shandong Analysis and Test Center in Ji'nan, China. ESI-MS spectra were recorded on an API 4000 spectrometer. All reactions were monitored by TLC using 0.25 mm silica gel plates (60GF-254). UV light and ferric chloride were used to visualize the spots. Silica gel was used for column chromatography purification. Flash chromatography was accomplished using the automated CombiFlash Rf system from Teledyne ISCO and was done using silica gel of 200–300 mesh. Melting points were determined on an electrothermal melting point apparatus. All tested compounds are >95% pure by HPLC analysis, performed on an Agilent 1100 HPLC instrument using an ODS HYPERSIL column (5  $\mu$ m, 4.6 mm  $\times$  250 mm) according to one of the following methods. Method A: compounds **10a**, **11a–11x**, and **27a–27c** were eluted with 35% acetonitrile/65% water (containing 0.4% formic acid)–65% acetonitrile/35% water (containing 0.4% formic acid) over 20 min, with detection at 290 nm and a flow rate of 1 mL/min. Method B: compounds **21a–21c** were eluted with 30% acetonitrile–70% 0.05 M potassium dihydrogen phosphate/phosphoric acid (PH = 3.0) over 20 min, with detection at 290 nm and a flow rate of 1 mL/min. The temperature of the column was 25  $^{\circ}$ C, and quantity of injection was 20  $\mu$ M.

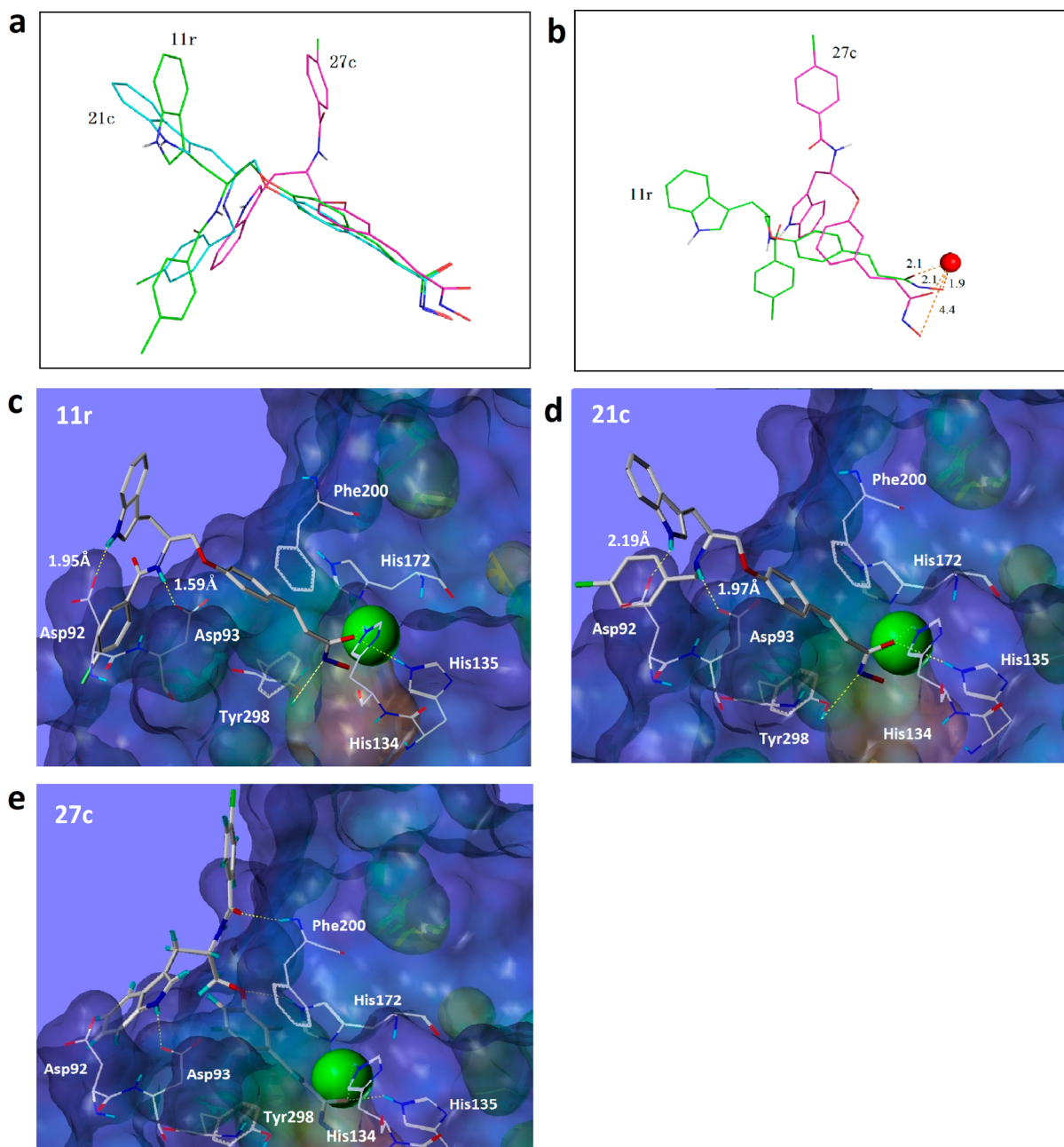


**Figure 8.** (a) Docked conformational alignment modeling of compounds **11r**, **21c**, and **27c**. For clarity, HDAC3 (derived by modification of PDB code 4A69 using Tripos SYBYL 8.0) used for docking is not shown. (b) Proposed docked mode of **27c** and **11r** for binding zinc. (c–e) Proposed binding preferences comparison of compounds **11r** (c), **21c** (d), and **27c** (e) at HDAC3. The zinc ion is shown as a red sphere, and the dashed lines stand for the hydrogen bonds (atom types: H, white; N, blue; O, red).

(*S*)-Methyl 2-amino-3-(1*H*-indol-3-yl)propanoate hydrochloride (**2**), (*S*)-Methyl 2-((*tert*-butoxycarbonyl)amino)-3-(1*H*-indol-3-yl)propanoate (**3**), and (*S*)-*tert*-butyl(1-hydroxy-3-(1*H*-indol-3-yl)propan-2-yl)carbamate (**4**) were synthesized as described previously.<sup>24</sup>

**General Procedure for the Preparation of 6 and 23.** (*E*)-Methyl 3-(4-hydroxyphenyl)acrylate. (**6**). *p*-Coumaric acid (16.4g, 100mmol) was dissolved in 200 mL of MeOH, then acetyl chloride (24g, 300mmol) was added dropwise at 0 °C; the mixed solution was refluxed at 75 °C for 5 h. The solvent was evaporated under vacuum; the product was dissolved with EtOAc, washed by saturated NaHCO<sub>3</sub> solution (2 × 100 mL), 1 M aqueous citric acid (2 × 100 mL), and brine (2 × 100 mL), dried over MgSO<sub>4</sub> overnight, and evaporated under vacuum to obtained product compound **6**, a white solid (15.6g, 87.5%). Mp: 140–141 °C. <sup>1</sup>H NMR (300 MHz, DMSO-*d*<sub>6</sub>) δ 3.69 (s,

3H), 6.43 (d, *J* = 16.2 Hz, 1H), 6.81 (d, *J* = 8.7 Hz, 2H), 7.54–7.59 (m, 3H), 10.01 (s, 1H). ESI-MS *m/z*: 179.2 [M + H]<sup>+</sup>.

(*E*)-Methyl 3-(4-Hydroxyphenyl)acrylate. (**23**). Mp: 90–91 °C. <sup>1</sup>H NMR (300 MHz, DMSO-*d*<sub>6</sub>) δ 3.72 (s, 1H), 6.54 (d, *J* = 15.9 Hz, 1H), 6.83–6.86 (m, 1H), 7.04–7.05 (m, 1H), 7.15 (d, *J* = 7.5 Hz, 1H), 7.20–7.25 (m, 1H), 7.60 (d, *J* = 15.9 Hz, 1H), 7.62 (s, 1H). ESI-MS *m/z*: 179.2 [M + H]<sup>+</sup>.

**General Procedure for the Preparation of 12.** *tert*-Butyl (1-Hydroxy-3-(1-methyl-1*H*-indol-3-yl)propan-2-yl)carbamate (**12**). Compound **4** (2.9g, 10mmol) was taken up in THF (50 mL), then (CH<sub>3</sub>CH<sub>2</sub>CH<sub>2</sub>CH<sub>2</sub>)<sub>4</sub>N(Br) (TBABr, 0.5g) was added followed by CH<sub>3</sub>I (3.5g, 25mmol). The reaction was stirred overnight, THF was evaporated under vacuum, and the residue was extracted with EtOAc (3 × 50 mL). The organic layer was washed with saturated NaHCO<sub>3</sub> solution (2 × 100 mL), 1 M aqueous citric acid (2 × 100 mL), and

brine (2 × 100 mL) and dried over MgSO<sub>4</sub> overnight. EtOAc was evaporated under vacuum. The crude product was purified by recrystallization with EtOAc and petroleum ether. The desired compound **12** was white solid (1.6g, 54% yield). Mp: 122–124 °C. <sup>1</sup>H NMR (300 MHz, DMSO-*d*<sub>6</sub>) δ 1.35 (s, 9H), 2.60–2.73 (m, 1H), 2.84–2.91 (m, 1H), 3.22–3.40 (m, 2H), 3.58–3.67 (m, 1H), 3.72 (s, 3H), 4.64 (t, *J* = 5.4 Hz, 1H), 6.53 (d, *J* = 8.1 Hz, 1H), 7.69–7.07 (m, 2H), 7.15 (t, *J* = 7.8 Hz, 1H), 7.37 (d, *J* = 8.1 Hz, 1H), 7.60 (d, *J* = 7.8 Hz, 1H). ESI-MS *m/z*: 305.5 [M + H]<sup>+</sup>.

**General Procedure for the Preparation of 7, 13, and 24.** (*S,E*)-Methyl 3-(4-(2-((*tert*-Butoxycarbonyl)amino)-3-(1*H*-indol-3-yl)propoxy)phenyl)acrylate (**7**). Compound **4** (5.8g, 20mmol), **6** (4.2g, 24mmol), and PPh<sub>3</sub> (7.9g, 30mmol) were dissolved in anhydrous THF, and then DEAD (5.2g, 30mmol) was added dropwise at 0 °C; the mixture was stirred for 4 h, and then THF was evaporated. The crude material was purified via flash chromatography to afford the compound **7**, a white solid (5.4g, 60%). Mp: 110–112 °C. <sup>1</sup>H NMR (300 MHz, DMSO-*d*<sub>6</sub>) δ 1.36 (s, 9H), 2.85–3.00 (m, 2H), 3.70 (s, 3H), 3.95–4.07 (m, 3H), 6.51 (d, *J* = 15.9 Hz, 1H), 6.93–6.99 (m, 4H), 7.08 (t, *J* = 7.4 Hz, 1H), 7.13 (d, *J* = 2.1 Hz, 1H), 7.34 (d, *J* = 7.8 Hz, 1H), 7.56 (d, *J* = 7.8 Hz, 1H), 7.63 (d, *J* = 15.9 Hz, 1H), 7.66 (d, *J* = 8.4 Hz, 2H), 10.82 (d, *J* = 1.5 Hz, 1H). ESI-MS *m/z*: 451.5 [M + H]<sup>+</sup>.

(*S,E*)-Methyl 3-(4-(2-((*tert*-Butoxycarbonyl)amino)-3-(1-methyl-1*H*-indol-3-yl)propoxy)phenyl)acrylate (**13**). Colorless oil crystallized upon standing, 50% yield.

(*S,E*)-Methyl 3-(3-(2-((*tert*-Butoxycarbonyl)amino)-3-(1*H*-indol-3-yl)propoxy)phenyl)acrylate (**24**). Colorless oil crystallized upon standing, 50% yield. ESI-MS *m/z*: 451.4 [M + H]<sup>+</sup>.

**General Procedure for the Preparation of 8 and 25.** (*S,E*)-Methyl 3-(4-(2-Amino-3-(1*H*-indol-3-yl)propoxy)phenyl)acrylate Hydrochloride (**8**). Compound **7** was dissolved in a solution of EtOAc (8 mL) saturated by dry HCl gas. The solution was stirred at room temperature overnight. The filtered precipitate was washed by diethyl ether to give the compound **8**, a white solid powder (3.8g, 83%). Mp: 198–200 °C. <sup>1</sup>H NMR (300 MHz, DMSO-*d*<sub>6</sub>) δ 3.10–3.24 (m, 2H), 3.71 (s, 3H), 3.71–3.75 (m, 1H), 4.07 (dd, *J* = 5.7 Hz, *J* = 10.5 Hz, 1H), 4.21 (dd, *J* = 5.7 Hz, *J* = 10.5 Hz, 1H), 6.53 (d, *J* = 15.9 Hz, 1H), 6.97–7.01 (m, 3H), 7.11 (t, *J* = 6.9 Hz, 1H), 7.27 (d, *J* = 2.4 Hz, 1H), 7.38 (d, *J* = 8.1 Hz, 1H), 7.59–7.64 (m, 2H), 7.70 (d, *J* = 8.7 Hz, 2H), 8.40 (s, 2H), 11.05 (s, 1H). ESI-MS *m/z*: 351.5 [M + H]<sup>+</sup>.

(*S,E*)-Methyl 3-(3-(2-Amino-3-(1*H*-indol-3-yl)propoxy)phenyl)acrylate Hydrochloride (**25**). Pale yellow oil. ESI-MS *m/z*: 351.5 [M + H]<sup>+</sup>.

**General Procedure for the Preparation of 9a–9y and 26a–26c.** (*S,E*)-Methyl 3-(4-(3-(1*H*-Indol-3-yl)-2-(4-methylphenylsulfonamido)propoxy)phenyl)acrylate (**9f**). To a solution of *p*-toluene sulfonic acid (0.34g, 2mmol) in anhydrous CH<sub>2</sub>Cl<sub>2</sub> was added 2-(1*H*-benzotriazole-1-yl)-1,1,3,3-tetramethyluronium tetrafluoroborate (TBTU, 0.71g, 2.2mmol), followed by Et<sub>3</sub>N (0.3g, 3mmol). After 30 min, compound **8** (0.85g, 2.2mmol) was added followed by TEA (0.3g, 3mmol). Four hours later, the solution of CH<sub>2</sub>Cl<sub>2</sub> was washed with 1 N HCl (2 × 30 mL), saturated Na<sub>2</sub>CO<sub>3</sub> (2 × 30 mL), and brine (2 × 30 mL), dried over MgSO<sub>4</sub> overnight, and the solvent was evaporated under vacuum. The crude product was purified by recrystallization with EtOAc and petroleum ether to achieve a white pure solid (0.51g, 50% yield). Mp: 72–74 °C. <sup>1</sup>H NMR (300 MHz, DMSO-*d*<sub>6</sub>) δ 2.30 (s, 3H), 2.85 (dd, *J* = 6.0 Hz, *J* = 14.4 Hz, 1H), 3.01 (dd, *J* = 8.1 Hz, *J* = 14.4 Hz, 1H), 3.60–3.65 (m, 1H), 3.70 (s, 3H), 3.86 (d, *J* = 4.8 Hz, 2H), 6.50 (d, *J* = 16.2 Hz, 1H), 6.76 (d, *J* = 8.7 Hz, 2H), 6.91 (t, *J* = 7.4 Hz, 1H), 7.00–7.06 (m, 2H), 7.20 (d, *J* = 8.1 Hz, 2H), 7.24–7.30 (m, 2H), 7.56–7.62 (m, 5H), 7.99 (d, *J* = 7.2 Hz, 1H), 10.77 (d, *J* = 1.5 Hz, 1H). ESI-MS *m/z*: 505.4 [M + H]<sup>+</sup>.

(*S,E*)-Methyl 3-(4-(2-(2-((*tert*-Butoxycarbonyl)amino)acetamido)-3-(1*H*-indol-3-yl)propoxy)phenyl)acrylate (**9a**). Colorless oil crystallized upon standing, 70% yield.

(*E*)-Methyl 3-(4-((*S*)-2-((*R*)-2-((*tert*-Butoxycarbonyl)amino)-4-(methylthio)butanamido)-3-(1*H*-indol-3-yl)propoxy)phenyl)acrylate (**9b**). Colorless oil crystallized upon standing, 73% yield.

(*E*)-Methyl 3-(4-((*S*)-2-((*R*)-2-((*tert*-Butoxycarbonyl)amino)-3-hydroxypropanamido)-3-(1*H*-indol-3-yl)propoxy)phenyl)acrylate (**9c**). Colorless oil crystallized upon standing, 75% yield.

(*E*)-Methyl 3-(4-((*2S*)-2-((*2R*)-2-((*tert*-Butoxycarbonyl)amino)-3-hydroxybutanamido)-3-(1*H*-indol-3-yl)propoxy)phenyl)acrylate (**9d**). Colorless oil crystallized upon standing, 70% yield.

(*S,E*)-Methyl 3-(4-(2-Benzamido-3-(1*H*-indol-3-yl)propoxy)phenyl)acrylate (**9e**). Colorless oil crystallized upon standing, 78% yield.

(*S,E*)-Methyl 3-(4-(2-([1,1'-Biphenyl]-4-ylcarboxamido)-3-(1*H*-indol-3-yl)propoxy)phenyl)acrylate (**9g**). Colorless oil crystallized upon standing, 76% yield. ESI-MS *m/z*: 531.4 [M + H]<sup>+</sup>.

(*S,E*)-Methyl 3-(4-(2-([1,1'-Biphenyl]-4-ylsulfonamido)-3-(1*H*-indol-3-yl)propoxy)phenyl)acrylate (**9h**). White solid, 76% yield. Mp: 148–150 °C. ESI-MS *m/z*: 567.5 [M + H]<sup>+</sup>.

(*S,E*)-Methyl 3-(4-(2-(2-Ethylbutanamido)-3-(1*H*-indol-3-yl)propoxy)phenyl)acrylate (**9i**). Colorless oil crystallized upon standing, 70% yield. ESI-MS *m/z*: 449.5 [M + H]<sup>+</sup>.

(*S,E*)-Methyl 3-(4-(3-(1*H*-Indol-3-yl)-2-(2-propylpentanamido)propoxy)phenyl)acrylate (**9j**). White pure solid, 70% yield. Mp: 170–172 °C. <sup>1</sup>H NMR (300 MHz, DMSO-*d*<sub>6</sub>) δ 0.73–0.80 (m, 6H), 0.96–1.00 (m, 2H), 1.04–1.11 (m, 4H), 1.30–1.42 (m, 2H), 2.10–2.17 (m, 1H), 2.86–3.03 (m, 2H), 3.70 (s, 3H), 3.98–4.07 (m, 2H), 4.34–4.42 (m, 1H), 6.51 (d, *J* = 15.9 Hz, 1H), 6.92–6.95 (m, 3H), 7.07 (t, *J* = 7.5 Hz, 1H), 7.14 (d, *J* = 2.4 Hz, 1H), 7.33 (d, *J* = 7.8 Hz, 1H), 7.58 (d, *J* = 9.0 Hz, 1H), 7.64 (d, *J* = 17.0 Hz, 1H), 7.67 (d, *J* = 9.0 Hz, 2H), 7.94 (d, *J* = 7.8 Hz, 1H), 10.82 (d, *J* = 1.5 Hz, 1H). ESI-MS *m/z*: 485.5 [M + H]<sup>+</sup>.

(*S,E*)-Methyl 3-(4-(2-(2-Hydroxybenzamido)-3-(1*H*-indol-3-yl)propoxy)phenyl)acrylate (**9k**). Colorless oil crystallized upon standing, 74% yield.

(*S,E*)-Methyl 3-(4-(2-(2-((2,3-Dimethylphenyl)amino)benzamido)-3-(1*H*-indol-3-yl)propoxy)phenyl)acrylate (**9l**). White pure solid, 76% yield. Mp: 84–86 °C. <sup>1</sup>H NMR (300 MHz, DMSO-*d*<sub>6</sub>) δ 2.08 (s, 3H), 3.27 (s, 3H), 3.08–3.16 (m, 2H), 3.70 (s, 3H), 4.11–4.22 (m, 2H), 4.55–4.64 (m, 1H), 6.49 (d, *J* = 15.9 Hz, 1H), 6.74 (t, *J* = 7.8 Hz, 1H), 6.83 (d, *J* = 7.8 Hz, 1H), 6.91–6.99 (m, 4H), 7.03–7.09 (m, 3H), 7.20–7.26 (m, 2H), 7.34 (d, *J* = 8.1 Hz, 1H), 7.57–7.64 (m, 5H), 8.57 (d, *J* = 7.8 Hz, 1H), 9.39 (s, 1H), 10.84 (d, *J* = 1.5 Hz, 1H). ESI-MS *m/z*: 574.5 [M + H]<sup>+</sup>.

(*E*)-Methyl 3-(4-((*2S*)-3-(1*H*-Indol-3-yl)-2-(2-(4-isobutylphenyl)propanamido)propoxy)phenyl)acrylate (**9m**). Colorless oil crystallized upon standing, 74% yield. ESI-MS *m/z*: 539.5 [M + H]<sup>+</sup>.

(*E*)-Methyl 3-(4-((*2S*)-2-(2-(4-Benzoylphenyl)propanamido)-3-(1*H*-indol-3-yl)propoxy)phenyl)acrylate (**9n**). Colorless oil crystallized upon standing, 73% yield. ESI-MS *m/z*: 563.4 [M + H]<sup>+</sup>.

(*E*)-Methyl 3-(4-((*S*)-3-(1*H*-Indol-3-yl)-2-((*S*)-2-(6-methoxynaphthalen-2-yl)propanamido)propoxy)phenyl)acrylate (**9o**). Colorless oil crystallized upon standing, 70% yield. ESI-MS *m/z*: 587.3 [M + H]<sup>+</sup>.

(*S,E*)-Methyl 3-(4-(3-(1*H*-Indol-3-yl)-2-(2-phenylacetamido)propoxy)phenyl)acrylate (**9p**). White pure solid, 60% yield. Mp: 154–156 °C. <sup>1</sup>H NMR (300 MHz, DMSO-*d*<sub>6</sub>) δ 2.90–3.06 (m, 2H), 3.43 (s, 2H), 3.71 (s, 3H), 4.01 (d, *J* = 5.4 Hz, 2H), 4.27–4.35 (m, 1H), 6.52 (d, *J* = 15.9 Hz, 1H), 6.91–6.96 (m, 3H), 7.08 (t, *J* = 7.5 Hz, 1H), 7.10 (d, *J* = 2.1 Hz, 1H), 7.17–7.27 (m, 5H), 7.34 (d, *J* = 8.1 Hz, 1H), 7.57 (d, *J* = 7.8 Hz, 1H), 7.64 (d, *J* = 16.2 Hz, 1H), 7.67 (d, *J* = 8.7 Hz, 2H), 8.30 (d, *J* = 7.8 Hz, 1H), 10.83 (d, *J* = 1.5 Hz, 1H). ESI-MS *m/z*: 470.5 [M + H]<sup>+</sup>.

(*S,E*)-Methyl 3-(4-(3-(1*H*-Indol-3-yl)-2-(3-phenylpropanamido)propoxy)phenyl)acrylate (**9q**). Colorless oil crystallized upon standing, 70% yield.

(*S,E*)-Methyl 3-(4-(2-(4-Chlorobenzamido)-3-(1*H*-indol-3-yl)propoxy)phenyl)acrylate (**9r**). Colorless oil crystallized upon standing, 75% yield. ESI-MS *m/z*: 489.4 [M + H]<sup>+</sup>.

(*S,E*)-Methyl 3-(4-(2-(2-Chlorobenzamido)-3-(1*H*-indol-3-yl)propoxy)phenyl)acrylate (**9s**). Colorless oil crystallized upon standing, 78% yield.

(*S,E*)-Methyl 3-(4-(2-(3-Chlorobenzamido)-3-(1*H*-indol-3-yl)propoxy)phenyl)acrylate (**9t**). Colorless oil crystallized upon standing, 77% yield.



(*S,E*)-Methyl 3-(4-(2-(2,4-Dichlorobenzamido)-3-(1*H*-indol-3-yl)propoxy)phenyl)acrylate (**9u**). Colorless oil crystallized upon standing, 70% yield.

(*S,E*)-Methyl 3-(4-(2-(3,4-Dichlorobenzamido)-3-(1*H*-indol-3-yl)propoxy)phenyl)acrylate (**9v**). Colorless oil crystallized upon standing, 68% yield.

(*S,E*)-Methyl 3-(4-(2-(4-Fluorobenzamido)-3-(1*H*-indol-3-yl)propoxy)phenyl)acrylate (**9w**). Colorless oil crystallized upon standing, 80% yield. ESI-MS  $m/z$ : 477.4 [M + H]<sup>+</sup>.

(*S,E*)-Methyl 3-(4-(2-(4-Bromobenzamido)-3-(1*H*-indol-3-yl)propoxy)phenyl)acrylate (**9x**). Colorless oil crystallized upon standing, 70% yield.

(*S,E*)-Methyl 3-(3-(2-Benzamido-3-(1*H*-indol-3-yl)propoxy)phenyl)acrylate (**26a**). Colorless oil crystallized upon standing, 65% yield.

(*S,E*)-Methyl 3-(3-(2-(4-Chlorobenzamido)-3-(1*H*-indol-3-yl)propoxy)phenyl)acrylate (**26b**). Colorless oil crystallized upon standing, 73% yield.

(*S,E*)-Methyl 3-(4-(2-(4-Fluorobenzamido)-3-(1*H*-indol-3-yl)propoxy)phenyl)acrylate (**26c**). Colorless oil crystallized upon standing, 70% yield.

**General Procedure for the Preparation of 18a–18c.** (*S,E*)-Methyl 3-(4-(2-(Benzylamino)-3-(1*H*-indol-3-yl)propoxy)phenyl)acrylate (**18a**). The solution of compound **8** (0.76g, 2mmol) in CH<sub>3</sub>OH was added Et<sub>3</sub>N (0.22g, 2mmol) for neutralization, followed by the addition of methanol (0.21g, 2mmol); the resulting solution was stirred for 2 h and the solvent evaporated. The residue was dissolved in anhydrous CH<sub>3</sub>OH, NaBH<sub>4</sub> (0.15g, 4mmol) was added slowly at 0 °C, the mixture was stirred at room temperature overnight, and after the reaction finished, the reaction was quenched by adding ice water slowly. CH<sub>3</sub>OH was evaporated, and the residue was extracted by EtOAc (3 × 30 mL). The organic layer was washed with brine (2 × 30 mL) and saturated Na<sub>2</sub>CO<sub>3</sub> (2 × 30 mL) and dried over MgSO<sub>4</sub> overnight. The solvent was evaporated under vacuum to get crude product **11a**, a colorless oil (0.79g, 90%). <sup>1</sup>H NMR (300 MHz, DMSO-*d*<sub>6</sub>) δ 2.95 (d, *J* = 6.3 Hz, 2H), 3.14–3.18 (m, 1H), 3.70 (s, 3H), 3.87 (s, 2H), 3.94 (d, *J* = 5.1 Hz, 2H), 6.50 (d, *J* = 15.9 Hz, 1H), 6.92 (t, *J* = 7.5 Hz, 1H), 6.95 (d, *J* = 8.7 Hz, 2H), 7.06 (t, *J* = 7.4 Hz, 1H), 7.14 (d, *J* = 2.4 Hz, 1H), 7.16–7.22 (m, 1H), 7.26–7.33 (m, 5H), 7.43 (d, *J* = 7.8 Hz, 1H), 7.63 (d, *J* = 15.9 Hz, 1H), 7.65 (d, *J* = 8.7 Hz, 2H), 8.99 (s, 1H), 10.83 (s, 1H). ESI-MS  $m/z$ : 441.5 [M + H]<sup>+</sup>.

(*S,E*)-Methyl 3-(4-(2-((4-Fluorobenzyl)amino)-3-(1*H*-indol-3-yl)propoxy)phenyl)acrylate (**18b**). Colorless oil, 85% yield.

(*S,E*)-methyl 3-(4-(2-((4-Chlorobenzyl)amino)-3-(1*H*-indol-3-yl)propoxy)phenyl)acrylate (**18c**). Colorless oil, 88% yield.

**General Procedure for the Preparation of 19a–19c.** (*S,E*)-Methyl 3-(4-(2-(Benzyl(tert-butoxycarbonyl)amino)-3-(1*H*-indol-3-yl)propoxy)phenyl)acrylate (**19a**). Et<sub>3</sub>N (0.61g, 6mmol) followed by (Boc)<sub>2</sub>O (0.78g, 3.6mmol) were added to the solution of compound **11a** (0.79g, 1.8mmol) in CH<sub>2</sub>Cl<sub>2</sub>. The reaction was stirred at room temperature overnight. The resulting solution was washed by saturated NaHCO<sub>3</sub> solution (2 × 30 mL), 1 M aqueous citric acid (2 × 30 mL), and brine (2 × 30 mL) and dried over MgSO<sub>4</sub> overnight. The solvent was evaporated under vacuum to get crude product **12a**, a colorless oil (0.92g, 95%). <sup>1</sup>H NMR (300 MHz, DMSO-*d*<sub>6</sub>) δ 1.43–1.47 (m, 9H), 2.90–3.16 (m, 2H), 3.70 (s, 3H), 4.00–4.07 (m, 2H), 4.31–4.37 (m, 2H), 4.56 (m, 1H), 6.49 (d, *J* = 16.2 Hz, 1H), 6.77–6.80 (m, 2H), 6.98 (t, *J* = 7.8 Hz, 1H), 7.09 (m, 2H), 7.12–7.17 (m, 1H), 7.20–7.24 (m, 4H), 7.35 (d, *J* = 7.8 Hz, 1H), 7.41–7.47 (m, 1H), 7.56–7.64 (m, 3H), 10.84 (s, 1H). ESI-MS  $m/z$ : 541.4 [M + H]<sup>+</sup>.

(*S,E*)-Methyl 3-(4-(2-((tert-Butoxycarbonyl)(4-fluorobenzyl)amino)-3-(1*H*-indol-3-yl)propoxy)phenyl)acrylate (**19b**). Colorless oil, 90% yield.

(*S,E*)-Methyl 3-(4-(2-((tert-Butoxycarbonyl)(4-chlorobenzyl)amino)-3-(1*H*-indol-3-yl)propoxy)phenyl)acrylate (**19c**). Colorless oil, 91% yield.

**General Procedure for the Preparation of 10a, 11a–11x, 14, 20a–20c, and 27a–27c.** (*S,E*)-*tert*-Butyl(1-(4-(3-(hydroxyamino)-3-oxoprop-1-en-1-yl)phenoxy)-3-(1*H*-indol-3-yl)propan-2-yl)carbamate (**10a**). KOH (28g, 509mmol) and NH<sub>2</sub>OH·HCl (23.5g,

343mmol) were dissolved, respectively, in 70 and 120 mL of MeOH to get solution A and solution B. Next, solution A was added dropwise to solution B. After filtering the precipitate (KCl), a NH<sub>2</sub>OK solution was obtained. Compound **7** (0.45g, 1 mmol) was dissolved in the NH<sub>2</sub>OK solution and stirred overnight. After the reaction was complete, it was evaporated under vacuum. The residue was acidified with 1 N HCl to a pH 3–4 and then extracted with EtOAc (3 × 20 mL). The organic layer was washed with brine (2 × 30 mL) and dried over Na<sub>2</sub>SO<sub>4</sub> overnight. The crude material was purified via flash chromatography to afford the compound **10a** (0.15g, 30% yield). Mp: 151–152 °C. <sup>1</sup>H NMR (300 MHz, DMSO-*d*<sub>6</sub>) δ 1.37 (s, 9H), 2.79–3.00 (m, 2H), 3.90–4.04 (m, 3H), 6.33 (d, *J* = 15.6 Hz, 1H), 6.92–7.00 (m, 4H), 7.08 (td, *J* = 0.9 Hz, *J* = 7.6 Hz, 1H), 7.13 (d, *J* = 1.8 Hz, 1H), 7.34 (d, *J* = 7.8 Hz, 1H), 7.42 (d, *J* = 15.6 Hz, 1H), 7.48 (d, *J* = 8.7 Hz, 2H), 7.56 (d, *J* = 7.8 Hz, 1H), 8.97 (s, 1H), 10.66 (s, 1H), 10.83 (d, *J* = 1.8 Hz, 1H). HRMS (AP-ESI)  $m/z$  calcd for C<sub>25</sub>H<sub>29</sub>N<sub>3</sub>O<sub>5</sub> [M + H]<sup>+</sup> 452.2180, found 452.2182. Retention time: 18.9 min, eluted with 40% acetonitrile/60% water (containing 0.4% formic acid).

(*S,E*)-*tert*-Butyl(2-((1-(4-(3-(hydroxyamino)-3-oxoprop-1-en-1-yl)phenoxy)-3-(1*H*-indol-3-yl)propan-2-yl)amino)-2-oxoethyl)carbamate (**11a**). Pale yellow solid, 34% yield. Mp: 72–74 °C. <sup>1</sup>H NMR (300 MHz, DMSO-*d*<sub>6</sub>) δ 1.39 (s, 9H), 2.85–3.10 (m, 2H), 3.48–3.57 (m, 2H), 3.96 (m, 2H), 4.31–4.35 (m, 1H), 6.33 (d, *J* = 15.9 Hz, 1H), 6.99–6.90 (m, 4H), 7.08 (t, *J* = 6.9 Hz, 1H), 7.14 (d, *J* = 2.1 Hz, 1H), 7.33 (d, *J* = 8.1 Hz, 1H), 7.42 (d, *J* = 15.9 Hz, 1H), 7.49 (d, *J* = 8.4 Hz, 2H), 7.59 (d, *J* = 7.8 Hz, 1H), 7.98 (d, *J* = 7.8 Hz, 1H), 8.98 (s, 1H), 10.66 (s, 1H), 10.85 (d, *J* = 1.8 Hz, 1H). HRMS (AP-ESI)  $m/z$  calcd for C<sub>27</sub>H<sub>32</sub>N<sub>4</sub>O<sub>6</sub> [M + H]<sup>+</sup> 509.2395, found 509.2392. Retention time: 7.4 min, eluted with 40% acetonitrile/60% water (containing 0.4% formic acid).

*tert*-Butyl((*R*)-1-(((*S*)-1-(4-((*E*)-3-(hydroxyamino)-3-oxoprop-1-en-1-yl)phenoxy)-3-(1*H*-indol-3-yl)propan-2-yl)amino)-4-(methylthio)-1-oxobutan-2-yl)carbamate (**11b**). Pale yellow solid, 30% yield. Mp: 108–110 °C. <sup>1</sup>H NMR (300 MHz, DMSO-*d*<sub>6</sub>) δ 1.37 (s, 9H), 1.68–1.82 (m, 2H), 2.42 (t, *J* = 7.8 Hz, 2H), 2.97–3.04 (m, 2H), 3.36 (s, 3H), 3.90–4.05 (m, 3H), 4.25–4.42 (m, 1H), 6.32 (d, *J* = 15.6 Hz, 1H), 6.90–6.97 (m, 4H), 7.08 (t, *J* = 6.9 Hz, 1H), 7.20 (d, *J* = 2.1 Hz, 1H), 7.34 (d, *J* = 7.8 Hz, 1H), 7.41 (d, 15.9 Hz, 1H), 7.48 (d, 8.4 Hz, 2H), 7.60 (d, *J* = 7.8 Hz, 1H), 7.99 (d, *J* = 7.5 Hz, 1H), 8.97 (s, 1H), 10.66 (s, 1H), 10.85 (s, 1H). HRMS (AP-ESI)  $m/z$  calcd for C<sub>30</sub>H<sub>38</sub>N<sub>4</sub>O<sub>6</sub>S [M + H]<sup>+</sup> 583.2585, found 583.2486. Retention time: 10.55 min, eluted with 47% acetonitrile/53% water (containing 0.4% formic acid).

*tert*-Butyl((*R*)-3-hydroxy-1-(((*S*)-1-(4-((*E*)-3-(hydroxyamino)-3-oxoprop-1-en-1-yl)phenoxy)-3-(1*H*-indol-3-yl)propan-2-yl)amino)-1-oxopropan-2-yl)carbamate (**11c**). Pale yellow solid, 34% yield. Mp: 118–120 °C. <sup>1</sup>H NMR (300 MHz, DMSO-*d*<sub>6</sub>) δ 1.36 (s, 9H), 2.91–3.05 (m, 2H), 3.51–3.54 (m, 2H), 3.93–4.02 (m, 3H), 4.31–4.38 (m, 1H), 4.84 (t, *J* = 6.3 Hz, 1H), 6.33 (d, *J* = 15.6 Hz, 1H), 6.65 (d, 8.1 Hz, 1H), 6.92–6.97 (m, 3H), 7.08 (t, *J* = 6.9 Hz, 1H), 7.16 (d, *J* = 2.1 Hz, 1H), 7.34 (d, *J* = 8.4 Hz, 1H), 7.42 (d, *J* = 15.9 Hz, 1H), 7.49 (d, *J* = 8.4 Hz, 2H), 7.59 (d, *J* = 7.8 Hz, 1H), 7.96 (d, *J* = 8.1 Hz, 1H), 8.98 (s, 1H), 10.66 (s, 1H), 10.85 (d, *J* = 1.5 Hz, 1H). HRMS (AP-ESI)  $m/z$  calcd for C<sub>28</sub>H<sub>34</sub>N<sub>4</sub>O<sub>7</sub> [M + H]<sup>+</sup> 539.2500, found 539.2496. Retention time: 5.3 min, eluted with 40% acetonitrile/60% water (containing 0.4% formic acid).

*tert*-Butyl((*2R*)-3-hydroxy-1-(((*S*)-1-(4-((*E*)-3-(hydroxyamino)-3-oxoprop-1-en-1-yl)phenoxy)-3-(1*H*-indol-3-yl)propan-2-yl)amino)-1-oxobutan-2-yl)carbamate (**11d**). Pale yellow solid, 29% yield. Mp: 102–104 °C. <sup>1</sup>H NMR (300 MHz, DMSO-*d*<sub>6</sub>) δ 1.01 (d, *J* = 5.7 Hz, 3H), 1.37 (s, 9H), 2.92–3.05 (m, 2H), 3.86–3.94 (m, 4H), 4.34–4.36 (m, 1H), 4.78 (d, *J* = 5.4 Hz, 1H), 6.27–6.35 (m, 2H), 6.91–6.97 (m, 3H), 7.08 (t, *J* = 7.2 Hz, 1H), 7.16 (d, *J* = 1.8 Hz, 1H), 7.31–7.48 (m, 4H), 7.60 (d, *J* = 7.8 Hz, 1H), 7.96 (d, *J* = 7.8 Hz, 1H), 8.96 (s, 1H), 10.65 (s, 1H), 10.83 (s, 1H). HRMS (AP-ESI)  $m/z$  calcd for C<sub>29</sub>H<sub>36</sub>N<sub>4</sub>O<sub>7</sub> [M + H]<sup>+</sup> 553.2657, found 553.2658. Retention time: 6.5 min, eluted with 40% acetonitrile/60% water (containing 0.4% formic acid).

(*S,E*)-*N*-(1-(4-(3-(Hydroxyamino)-3-oxoprop-1-en-1-yl)phenoxy)-3-(1*H*-indol-3-yl)propan-2-yl)benzamide (**11e**). Pale yellow solid, 31% yield. Mp: 164–166 °C. <sup>1</sup>H NMR (300 MHz, DMSO-*d*<sub>6</sub>) δ 3.12

(d,  $J = 6.6$  Hz, 2H), 4.04–4.21 (m, 2H), 4.54–4.65 (m, 1H), 6.33 (d,  $J = 15.9$  Hz, 1H), 6.93–6.99 (m, 3H), 7.08 (td,  $J = 0.9$  Hz,  $J = 7.4$  Hz, 1H), 7.19 (d,  $J = 2.1$  Hz, 1H), 7.34 (d,  $J = 8.1$  Hz, 1H), 7.42 (d,  $J = 15.9$  Hz, 1H), 7.43–7.55 (m, 5H), 7.64 (d,  $J = 7.8$  Hz, 1H), 7.85 (d,  $J = 7.5$  Hz, 2H), 8.53 (d,  $J = 7.8$  Hz, 1H), 8.98 (s, 1H), 10.66 (s, 1H), 10.83 (d,  $J = 1.8$  Hz, 1H). HRMS (AP-ESI)  $m/z$  calcd for  $C_{27}H_{25}N_3O_4$   $[M + H]^+$  456.1918, found 456.1916. Retention time: 12.6 min, eluted with 40% acetonitrile/60% water (containing 0.4% formic acid).

(*S,E*)-3-(4-(3-(1*H*-Indol-3-yl)-2-(4-methylphenylsulfonamido)propoxy)phenyl)-*N*-hydroxyacrylamide (**11f**). Pale yellow solid, 34% yield. Mp: 118–120 °C.  $^1H$  NMR (300 MHz, DMSO- $d_6$ )  $\delta$  2.31 (s, 3H), 2.85 (dd,  $J = 6.0$  Hz,  $J = 14.4$  Hz, 1H), 3.01 (dd,  $J = 8.1$  Hz,  $J = 14.4$  Hz, 1H), 3.60–3.62 (m, 1H), 3.84 (d,  $J = 4.8$  Hz, 2H), 6.32 (d,  $J = 15.9$  Hz, 1H), 6.76 (d,  $J = 8.7$  Hz, 2H), 6.92 (td,  $J = 0.9$  Hz,  $J = 7.4$  Hz, 1H), 7.00–7.06 (m, 2H), 7.21 (d,  $J = 8.1$  Hz, 2H), 7.27 (d,  $J = 10.2$  Hz, 1H), 7.30 (d,  $J = 8.1$  Hz, 1H), 7.41 (d,  $J = 15.9$  Hz, 1H), 7.44 (d,  $J = 8.7$  Hz, 2H), 7.59 (d,  $J = 8.4$  Hz, 2H), 8.00 (d,  $J = 6.9$  Hz, 1H), 8.99 (s, 1H), 10.66 (s, 1H), 10.78 (d,  $J = 1.8$  Hz, 1H). HRMS (AP-ESI)  $m/z$  calcd for  $C_{27}H_{27}N_3O_5S$   $[M + H]^+$  506.1715, found 506.1744. Retention time: 22.9 min, eluted with 40% acetonitrile/60% water (containing 0.4% formic acid).

(*S,E*)-*N*-(1-(4-(3-(Hydroxyamino)-3-oxoprop-1-en-1-yl)phenoxy)-3-(1*H*-indol-3-yl)propan-2-yl)-[1,1'-biphenyl]-4-carboxamide (**11g**). Pale yellow solid, 30% yield. Mp: 174–176 °C.  $^1H$  NMR (300 MHz, DMSO- $d_6$ )  $\delta$  3.14 (d,  $J = 6.9$  Hz, 2H), 3.99–4.12 (m, 1H), 4.18–4.28 (m, 1H), 4.56–4.67 (m, 1H), 6.33 (d,  $J = 15.9$  Hz, 1H), 6.94–7.00 (m, 3H), 7.09 (t,  $J = 7.2$  Hz, 1H), 7.20 (d,  $J = 2.1$  Hz, 1H), 7.35 (d,  $J = 8.1$  Hz, 1H), 7.37–7.43 (m, 2H), 7.47–7.52 (m, 4H), 7.66 (d,  $J = 7.8$  Hz, 1H), 7.72–7.78 (m, 4H), 7.96 (d,  $J = 8.4$  Hz, 2H), 8.60 (d,  $J = 6.9$  Hz, 1H), 10.67 (s, 1H), 10.84 (s, 1H). HRMS (AP-ESI)  $m/z$  calcd for  $C_{33}H_{29}N_3O_4$   $[M + H]^+$  532.2192, found 532.2231. Retention time: 5.0 min, eluted with 40% acetonitrile/60% water (containing 0.4% formic acid).

(*S,E*)-3-(4-(2-([1,1'-Biphenyl]-4-ylsulfonamido)-3-(1*H*-indol-3-yl)propoxy)phenyl)-*N*-hydroxyacrylamide (**11h**). Pale yellow solid, 28% yield. Mp: 167–169 °C.  $^1H$  NMR (300 MHz, DMSO- $d_6$ )  $\delta$  2.85–2.91 (m, 1H), 2.98–3.05 (m, 1H), 3.64–3.75 (m, 1H), 3.82–3.91 (m, 1H), 6.29 (d,  $J = 15.9$  Hz, 1H), 6.75 (d,  $J = 8.7$  Hz, 2H), 6.91 (t,  $J = 7.8$  Hz, 1H), 7.01 (t,  $J = 7.8$  Hz, 1H), 7.10 (d,  $J = 2.1$  Hz, 1H), 7.24 (d,  $J = 8.1$  Hz, 1H), 7.30–7.45 (m, 5H), 7.48–7.53 (m, 2H), 7.64–7.68 (m, 4H), 7.77 (d,  $J = 8.4$  Hz, 2H), 8.17 (d,  $J = 7.2$  Hz, 1H), 8.99 (s, 1H), 10.65 (s, 1H), 10.80 (d,  $J = 1.8$  Hz, 1H). HRMS (AP-ESI)  $m/z$  calcd for  $C_{32}H_{29}N_3O_5S$   $[M + H]^+$  568.1861, found 568.1901. Retention time: 5.1 min, eluted with 65% acetonitrile/35% water (containing 0.4% formic acid).

(*S,E*)-2-Ethyl-*N*-(1-(4-(3-(hydroxyamino)-3-oxoprop-1-en-1-yl)phenoxy)-3-(1*H*-indol-3-yl)propan-2-yl)butanamide (**11i**). Pale yellow solid, 31% yield. Mp: 170–172 °C.  $^1H$  NMR (300 MHz, DMSO- $d_6$ )  $\delta$  0.69 (t,  $J = 7.2$  Hz, 3H), 0.79 (t,  $J = 7.5$  Hz, 3H), 1.23–1.47 (m, 4H), 1.91–2.02 (m, 1H), 2.90–3.04 (m, 2H), 3.99 (d,  $J = 5.4$  Hz, 2H), 4.36–4.44 (m, 1H), 6.33 (d,  $J = 15.9$  Hz, 1H), 6.95 (d, 8.4 Hz, 2H), 6.98 (td,  $J = 0.9$  Hz,  $J = 7.1$  Hz, 1H), 7.08 (td,  $J = 0.9$  Hz,  $J = 7.6$  Hz, 1H), 7.14 (d,  $J = 2.1$  Hz, 1H), 7.33 (d,  $J = 8.1$  Hz, 1H), 7.42 (d,  $J = 15.6$  Hz, 1H), 7.49 (d,  $J = 8.4$  Hz, 2H), 7.59 (d,  $J = 7.8$  Hz, 1H), 7.97 (d,  $J = 8.1$  Hz, 1H), 8.97 (s, 1H), 10.66 (s, 1H), 10.82 (d,  $J = 1.5$  Hz, 1H). HRMS (AP-ESI)  $m/z$  calcd for  $C_{26}H_{31}N_3O_4$   $[M + H]^+$  450.2387, found 450.2389. Retention time: 10.9 min, eluted with 40% acetonitrile/60% water (containing 0.4% formic acid).

(*S,E*)-*N*-(1-(4-(3-(Hydroxyamino)-3-oxoprop-1-en-1-yl)phenoxy)-3-(1*H*-indol-3-yl)propan-2-yl)-2-propylpentanamide (**11j**). Pale yellow solid, 27% yield. Mp: 171–172 °C.  $^1H$  NMR (300 MHz, DMSO- $d_6$ )  $\delta$  0.73–0.80 (m, 6H), 1.97–1.20 (m, 6H), 1.30–1.46 (m, 2H), 2.12–2.18 (m, 1H), 2.86–3.03 (m, 2H), 3.98 (d,  $J = 5.1$  Hz, 2H), 4.34–4.42 (m, 1H), 6.33 (d,  $J = 15.9$  Hz, 1H), 6.95 (d,  $J = 8.7$  Hz, 2H), 6.98 (td,  $J = 0.9$  Hz,  $J = 6.8$  Hz, 1H), 7.08 (td,  $J = 0.9$  Hz,  $J = 7.2$  Hz, 1H), 7.14 (d,  $J = 2.1$  Hz, 1H), 7.33 (d,  $J = 7.8$  Hz, 1H), 7.42 (d,  $J = 15.6$  Hz, 1H), 7.49 (d,  $J = 8.7$  Hz, 2H), 7.58 (d,  $J = 7.8$  Hz, 1H), 7.63 (d,  $J = 9.0$  Hz, 1H), 7.94 (d,  $J = 8.1$  Hz, 1H), 10.66 (s, 1H), 10.83 (d,  $J = 1.5$  Hz, 1H). HRMS (AP-ESI)  $m/z$  calcd for  $C_{28}H_{35}N_3O_4$   $[M + H]^+$

478.2699, found 478.2699. Retention time: 24.5 min, eluted with 40% acetonitrile/60% water (containing 0.4% formic acid).

(*S,E*)-2-Hydroxy-*N*-(1-(4-(3-(hydroxyamino)-3-oxoprop-1-en-1-yl)phenoxy)-3-(1*H*-indol-3-yl)propan-2-yl)benzamide (**11k**). Pale yellow solid, 35% yield. Mp: 120–122 °C.  $^1H$  NMR (300 MHz, DMSO- $d_6$ )  $\delta$  3.14 (d,  $J = 6.9$ , 2H), 4.08–4.22 (m, 2H), 4.59–4.70 (m, 1H), 6.33 (d,  $J = 15.9$  Hz, 1H), 6.86–6.91 (m, 2H), 6.96–7.00 (m, 3H), 7.09 (t,  $J = 7.4$  Hz, 1H), 7.18 (d,  $J = 2.1$  Hz, 1H), 7.35 (d,  $J = 8.1$  Hz, 1H), 7.37–7.42 (m, 2H), 7.49 (d,  $J = 8.4$  Hz, 2H), 7.64 (d,  $J = 7.8$  Hz, 1H), 7.92 (dd,  $J = 1.5$  Hz,  $J = 8.1$  Hz, 1H), 8.87 (d,  $J = 8.1$  Hz, 1H), 8.98 (s, 1H), 10.66 (s, 1H), 10.85 (d,  $J = 1.8$  Hz, 1H), 12.37 (s, 1H). HRMS (AP-ESI)  $m/z$  calcd for  $C_{27}H_{25}N_3O_5$   $[M + H]^+$  472.1867, found 472.1868. Retention time: 17.2 min, eluted with 40% acetonitrile/60% water (containing 0.4% formic acid).

(*S,E*)-2-(2-(3-Dimethylphenylamino)-*N*-(1-(4-(3-(hydroxyamino)-3-oxoprop-1-en-1-yl)phenoxy)-3-(1*H*-indol-3-yl)propan-2-yl)benzamide (**11l**). Pale yellow solid, 33% yield. Mp: 126–128 °C.  $^1H$  NMR (300 MHz, DMSO- $d_6$ )  $\delta$  2.08 (s, 3H), 2.27 (s, 3H), 3.05–3.12 (m, 2H), 4.08–4.20 (m, 2H), 4.55–4.67 (m, 1H), 6.32 (d,  $J = 15.9$  Hz, 1H), 6.74 (t,  $J = 7.5$  Hz, 1H), 6.83 (d,  $J = 8.4$  Hz, 1H), 6.91–6.98 (m, 4H), 7.03–7.09 (m, 3H), 7.23–7.26 (m, 2H), 7.34 (d,  $J = 8.1$  Hz, 1H), 7.41 (d,  $J = 15.9$  Hz, 1H), 7.47 (d,  $J = 8.1$  Hz, 2H), 7.64 (t,  $J = 7.2$  Hz, 2H), 8.58 (d,  $J = 8.1$  Hz, 1H), 8.97 (s, 1H), 9.40 (s, 1H), 10.65 (s, 1H), 10.84 (d,  $J = 1.5$  Hz, 1H). HRMS (AP-ESI)  $m/z$  calcd for  $C_{35}H_{34}N_4O_4$   $[M + H]^+$  534.1023, found 575.2653. Retention time: 10.2 min, eluted with 40% acetonitrile/60% water (containing 0.4% formic acid).

(*E*)-3-(4-(2*S*)-3-(1*H*-Indol-3-yl)-2-(2-(4-isobutylphenyl)propanamido)propoxy)phenyl)-*N*-hydroxyacrylamide (**11m**). Pale yellow solid, 30% yield. Mp: 116–118 °C.  $^1H$  NMR (300 MHz, DMSO- $d_6$ )  $\delta$  0.81–0.86 (m, 6H), 1.24–1.31 (m, 3H), 1.71–1.85 (m, 1H), 2.35–2.41 (m, 2H), 2.84–3.05 (m, 2H), 3.59–3.62 (m, 1H), 3.92 (m, 1H), 3.96–3.98 (m, 1H), 4.26–4.36 (m, 1H), 6.33 (dd,  $J = 4.5$  Hz,  $J = 15.9$  Hz, 1H), 6.84–7.08 (m, 6H), 7.13–7.19 (m, 3H), 7.42–7.61 (m, 5H), 8.14 (t,  $J = 6.4$  Hz, 1H), 8.97 (s, 1H), 10.66 (s, 1H), 10.83 (s, 1H). HRMS (AP-ESI)  $m/z$  calcd for  $C_{33}H_{37}N_3O_4$   $[M + H]^+$  540.2857, found 540.2856. Retention time: 7.7 min, eluted with 40% acetonitrile/60% water (containing 0.4% formic acid).

(*E*)-3-(4-(*S*)-3-(1*H*-Indol-3-yl)-2-(*S*)-2-(6-methoxyphthalen-2-yl)propanamido)propoxy)phenyl)-*N*-hydroxyacrylamide (**11o**). Pale yellow solid, 29% yield. Mp: 134–136 °C.  $^1H$  NMR (300 MHz, DMSO- $d_6$ )  $\delta$  1.35–1.42 (m, 3H), 2.89–3.08 (m, 2H), 3.74–3.80 (m, 1H), 3.85–3.86 (m, 3H), 3.92–4.00 (m, 2H), 4.29–4.39 (m, 1H), 6.31 (d,  $J = 15.9$  Hz, 1H), 6.84 (d,  $J = 8.7$  Hz, 2H), 6.94–7.09 (m, 3H), 7.11–7.51 (m, 8H), 7.62 (d,  $J = 7.8$  Hz, 1H), 7.67–7.75 (m, 3H), 8.23 (d,  $J = 7.8$  Hz, 1H), 8.98 (s, 1H), 10.66 (s, 1H), 10.85 (s, 1H). HRMS (AP-ESI)  $m/z$  calcd for  $C_{36}H_{33}N_3O_5$   $[M + H]^+$  564.2493, found 564.2495.

(*S,E*)-3-(4-(3-(1*H*-Indol-3-yl)-2-(2-phenylacetamido)propoxy)phenyl)-*N*-hydroxyacrylamide (**11p**). Pale yellow solid, 29% yield. Mp: 154–156 °C.  $^1H$  NMR (300 MHz, DMSO- $d_6$ )  $\delta$  2.90–3.06 (m, 2H), 3.43 (s, 2H), 3.99 (d,  $J = 5.1$  Hz, 2H), 4.27–4.38 (m, 1H), 6.34 (d,  $J = 15.9$  Hz, 1H), 6.91–6.97 (m, 3H), 7.08 (td,  $J = 0.9$ ,  $J = 7.4$  Hz, 1H), 7.11 (d,  $J = 2.1$  Hz, 1H), 7.17–7.28 (m, 5H), 7.35 (d,  $J = 8.1$  Hz, 1H), 7.42 (d,  $J = 15.9$  Hz, 1H), 7.50 (d,  $J = 8.7$  Hz, 2H), 7.58 (d,  $J = 7.8$  Hz, 1H), 8.31 (d,  $J = 7.8$  Hz, 1H), 8.99 (s, 1H), 10.66 (s, 1H), 10.84 (d,  $J = 1.5$  Hz, 1H). HRMS (AP-ESI)  $m/z$  calcd for  $C_{28}H_{27}N_3O_4$   $[M + H]^+$  470.2074, found 470.2074. Retention time: 12.8 min, eluted with 40% acetonitrile/60% water (containing 0.4% formic acid).

(*S,E*)-3-(4-(3-(1*H*-Indol-3-yl)-2-(3-phenylpropanamido)propoxy)phenyl)-*N*-hydroxyacrylamide (**11q**). Pale yellow solid, 30% yield. Mp: 166–168 °C.  $^1H$  NMR (300 MHz, DMSO- $d_6$ )  $\delta$  2.41 (t,  $J = 8.1$  Hz, 2H), 2.81 (t,  $J = 7.8$  Hz, 2H), 2.85–3.02 (m, 2H), 3.94 (d,  $J = 5.1$  Hz, 2H), 4.28–4.38 (m, 1H), 6.33 (d,  $J = 15.9$  Hz, 1H), 6.96 (d,  $J = 8.7$  Hz, 2H), 6.07 (t,  $J = 6.9$  Hz, 1H), 7.03–7.09 (m, 2H), 7.13–7.35 (m, 5H), 7.34 (d,  $J = 7.8$  Hz, 1H), 7.42 (d,  $J = 15.9$  Hz, 1H), 7.50 (d,  $J = 8.7$  Hz, 2H), 7.58 (d,  $J = 7.8$  Hz, 1H), 8.06 (d,  $J = 8.1$  Hz, 1H), 8.99 (s, 1H), 10.67 (s, 1H), 10.83 (d,  $J = 1.8$  Hz, 1H). HRMS (AP-ESI)  $m/z$  calcd for  $C_{29}H_{29}N_3O_4$   $[M + H]^+$  484.2236, found 484.2231.



Retention time: 17.4 min, eluted with 40% acetonitrile/60% water (containing 0.4% formic acid).

(*S,E*)-4-Chloro-*N*-(1-(4-(3-(hydroxyamino)-3-oxoprop-1-en-1-yl)phenoxy)-3-(1*H*-indol-3-yl)propan-2-yl)benzamide (**11r**). Pale yellow solid, 32% yield. Mp: 182–184 °C. <sup>1</sup>H NMR (300 MHz, DMSO-*d*<sub>6</sub>) δ 3.11 (d, *J* = 6.6 Hz, 2H), 4.06–4.11 (m, 1H), 4.14–4.20 (m, 1H), 4.54–4.61 (m, 1H), 6.32 (d, *J* = 15.6 Hz, 1H), 6.93–6.98 (m, 3H), 7.08 (t, *J* = 6.9 Hz, 1H), 7.18 (d, *J* = 2.1 Hz, 1H), 7.34 (d, *J* = 7.8 Hz, 1H), 7.42 (d, *J* = 15.9 Hz, 1H), 7.49 (d, *J* = 8.4 Hz, 2H), 7.55 (d, *J* = 8.7 Hz, 2H), 7.63 (d, *J* = 7.8 Hz, 1H), 7.88 (d, *J* = 8.7 Hz, 2H), 8.63 (d, *J* = 7.8 Hz, 1H), 8.98 (s, 1H), 10.66 (s, 1H), 10.83 (d, *J* = 1.5 Hz, 1H). HRMS (AP-ESI) *m/z* calcd for C<sub>27</sub>H<sub>24</sub>ClN<sub>3</sub>O<sub>4</sub> [M + H]<sup>+</sup> 490.1526, found 490.1528. Retention time: 6.0 min, eluted with 40% acetonitrile/60% water (containing 0.4% formic acid).

(*S,E*)-2-Chloro-*N*-(1-(4-(3-(hydroxyamino)-3-oxoprop-1-en-1-yl)phenoxy)-3-(1*H*-indol-3-yl)propan-2-yl)benzamide (**11s**). Pale yellow solid, 35% yield. Mp: 113–115 °C. <sup>1</sup>H NMR (300 MHz, DMSO-*d*<sub>6</sub>) δ 3.00–3.13 (m, 2H), 4.10 (d, *J* = 5.4 Hz, 2H), 4.49–4.57 (m, 1H), 6.33 (d, *J* = 15.9 Hz, 1H), 6.95–7.00 (m, 3H), 7.10 (t, *J* = 7.4 Hz, 1H), 7.22 (d, *J* = 2.1 Hz, 1H), 7.29 (dd, *J* = 1.8 Hz, *J* = 7.5 Hz, 1H), 7.32–7.40 (m, 3H), 7.42–7.50 (m, 4H), 7.63 (d, *J* = 7.8 Hz, 1H), 8.66 (d, *J* = 8.1 Hz, 1H), 8.98 (s, 1H), 10.67 (s, 1H), 10.87 (d, *J* = 1.8 Hz, 1H). HRMS (AP-ESI) *m/z* calcd for C<sub>27</sub>H<sub>24</sub>ClN<sub>3</sub>O<sub>4</sub> [M + H]<sup>+</sup> 490.1528, found 490.1528. Retention time: 10.8 min, eluted with 40% acetonitrile/60% water (containing 0.4% formic acid).

(*S,E*)-3-Chloro-*N*-(1-(4-(3-(hydroxyamino)-3-oxoprop-1-en-1-yl)phenoxy)-3-(1*H*-indol-3-yl)propan-2-yl)benzamide (**11t**). Pale yellow solid, 33% yield. Mp: 148–149 °C. <sup>1</sup>H NMR (300 MHz, DMSO-*d*<sub>6</sub>) δ 3.13 (d, *J* = 6.9 Hz, 2H), 4.06–4.11 (m, 1H), 4.14–4.21 (m, 1H), 4.54–4.65 (m, 1H), 6.48 (d, *J* = 15.9 Hz, 1H), 6.94–6.99 (m, 2H), 7.03–7.08 (m, 1H), 7.12–7.19 (m, 2H), 7.27–7.32 (m, 2H), 7.34–7.55 (m, 4H), 7.65 (d, *J* = 7.8 Hz, 1H), 7.83–7.85 (m, 2H), 8.53 (d, *J* = 8.1 Hz, 1H), 9.06 (s, 1H), 10.72 (s, 1H), 10.83 (s, 1H). HRMS (AP-ESI) *m/z* calcd for C<sub>27</sub>H<sub>24</sub>ClN<sub>3</sub>O<sub>4</sub> [M + H]<sup>+</sup> 490.1528, found 490.1528. Retention time: 18.8 min, eluted with 40% acetonitrile/60% water (containing 0.4% formic acid).

(*S,E*)-2,4-Dichloro-*N*-(1-(4-(3-(hydroxyamino)-3-oxoprop-1-en-1-yl)phenoxy)-3-(1*H*-indol-3-yl)propan-2-yl)benzamide (**11u**). Pale yellow solid, 29% yield. Mp: 159–160 °C. <sup>1</sup>H NMR (300 MHz, DMSO-*d*<sub>6</sub>) δ 3.03–3.16 (m, 2H), 4.10–4.19 (m, 2H), 4.51–4.60 (m, 1H), 6.33 (d, *J* = 15.6 Hz, 1H), 6.93–6.99 (m, 3H), 7.08 (t, *J* = 6.9 Hz, 1H), 7.18 (d, *J* = 2.1 Hz, 1H), 7.34 (d, *J* = 7.8 Hz, 1H), 7.42 (d, *J* = 15.9 Hz, 1H), 7.49 (d, *J* = 8.7 Hz, 2H), 7.63 (d, *J* = 7.8 Hz, 1H), 7.81 (d, *J* = 1.8 Hz, 2H), 7.83 (d, *J* = 1.8 Hz, 1H), 8.77 (d, *J* = 7.8 Hz, 1H), 8.97 (s, 1H), 10.66 (s, 1H), 10.85 (d, *J* = 1.5 Hz, 1H). HRMS (AP-ESI) *m/z* calcd for C<sub>27</sub>H<sub>23</sub>Cl<sub>2</sub>N<sub>3</sub>O<sub>4</sub> [M + H]<sup>+</sup> 534.1023, found 524.1138. Retention time: 10.1 min, eluted with 51% acetonitrile/49% water (containing 0.4% formic acid).

(*S,E*)-3,4-Dichloro-*N*-(1-(4-(3-(hydroxyamino)-3-oxoprop-1-en-1-yl)phenoxy)-3-(1*H*-indol-3-yl)propan-2-yl)benzamide (**11v**). Pale yellow solid, 30% yield. Mp: 162–164 °C. <sup>1</sup>H NMR (300 MHz, DMSO-*d*<sub>6</sub>) δ 3.00–3.13 (m, 2H), 4.08–4.10 (m, 2H), 4.47–4.58 (m, 1H), 6.33 (d, *J* = 15.9 Hz, 1H), 6.95–6.99 (m, 3H), 7.10 (t, *J* = 7.2 Hz, 1H), 7.21 (d, *J* = 2.1 Hz, 1H), 7.31 (d, *J* = 8.1 Hz, 1H), 7.36 (d, *J* = 8.1 Hz, 1H), 7.42 (d, *J* = 15.9 Hz, 1H), 7.48 (dd, *J* = 2.1 Hz, *J* = 8.1 Hz, 1H), 7.50 (d, *J* = 8.2 Hz, 2H), 7.63 (d, *J* = 7.8 Hz, 1H), 7.67 (d, *J* = 2.1 Hz, 1H), 8.72 (d, *J* = 8.1 Hz, 1H), 8.99 (s, 1H), 10.66 (s, 1H), 10.86 (s, 1H). HRMS (AP-ESI) *m/z* calcd for C<sub>27</sub>H<sub>23</sub>Cl<sub>2</sub>N<sub>3</sub>O<sub>4</sub> [M + H]<sup>+</sup> 524.1138, found 524.1138. Retention time: 14.2 min, eluted with 43% acetonitrile/57% water (containing 0.4% formic acid).

(*S,E*)-4-Fluoro-*N*-(1-(4-(3-(hydroxyamino)-3-oxoprop-1-en-1-yl)phenoxy)-3-(1*H*-indol-3-yl)propan-2-yl)benzamide (**11w**). Pale yellow solid, 27% yield. Mp: 180–182 °C. <sup>1</sup>H NMR (300 MHz, DMSO-*d*<sub>6</sub>) δ 3.11 (d, *J* = 6.9 Hz, 2H), 4.05–4.20 (m, 2H), 4.52–4.60 (m, 1H), 6.32 (d, *J* = 15.9 Hz, 1H), 6.93–6.99 (m, 3H), 7.08 (t, *J* = 6.9 Hz, 1H), 7.18 (d, *J* = 2.1 Hz, 1H), 7.26–7.33 (m, 3H), 7.41 (d, *J* = 15.9 Hz, 1H), 7.49 (d, *J* = 8.7 Hz, 2H), 7.63 (d, *J* = 7.8 Hz, 1H), 7.89–7.94 (m, 2H), 8.56 (d, *J* = 7.8 Hz, 1H), 8.98 (s, 1H), 10.66 (s, 1H), 10.83 (d, *J* = 1.5 Hz, 1H). HRMS (AP-ESI) *m/z* calcd for C<sub>27</sub>H<sub>24</sub>FN<sub>3</sub>O<sub>4</sub> [M

+ H]<sup>+</sup> 474.1824, found 474.1824. Retention time: 12.0 min, eluted with 40% acetonitrile/60% water (containing 0.4% formic acid).

(*S,E*)-4-Bromo-*N*-(1-(4-(3-(hydroxyamino)-3-oxoprop-1-en-1-yl)phenoxy)-3-(1*H*-indol-3-yl)propan-2-yl)benzamide (**11x**). Pale yellow solid, 32% yield. Mp: 182–184 °C. <sup>1</sup>H NMR (300 MHz, DMSO-*d*<sub>6</sub>) δ 3.11 (d, *J* = 6.9 Hz, 2H), 4.06–4.20 (m, 2H), 4.51–4.61 (m, 1H), 6.32 (d, *J* = 15.6 Hz, 1H), 6.93–6.98 (m, 3H), 7.08 (td, *J* = 0.9, *J* = 7.8 Hz, 1H), 7.17 (d, *J* = 2.1 Hz, 1H), 7.36 (d, *J* = 8.1 Hz, 1H), 7.41 (d, *J* = 15.6 Hz, 1H), 7.49 (d, *J* = 8.4 Hz, 2H), 7.66 (d, *J* = 9.3 Hz, 1H), 7.69 (d, *J* = 1.8 Hz, 2H), 7.81 (d, *J* = 1.8 Hz, 2H), 8.63 (d, *J* = 7.8 Hz, 1H), 8.98 (s, 1H), 10.66 (s, 1H), 10.83 (d, *J* = 1.8 Hz, 1H). HRMS (AP-ESI) *m/z* calcd for C<sub>27</sub>H<sub>24</sub>BrN<sub>3</sub>O<sub>4</sub> [M + H]<sup>+</sup> 534.1023, found 534.1021.

(*S,E*)-4-Methoxy-*N*-(1-(4-(3-(hydroxyamino)-3-oxoprop-1-en-1-yl)phenoxy)-3-(1*H*-indol-3-yl)propan-2-yl)benzamide (**11y**). Mp: 180–182 °C. <sup>1</sup>H NMR (300 MHz, DMSO-*d*<sub>6</sub>) δ 3.10 (d, *J* = 6.9 Hz, 2H), 3.80 (s, 3H), 4.02–4.20 (m, 2H), 4.52–4.63 (m, 1H), 6.33 (d, *J* = 15.9 Hz, 1H), 6.93–7.00 (m, 5H), 7.08 (td, *J* = 0.9 Hz, *J* = 7.4 Hz, 1H), 7.17 (d, *J* = 2.1 Hz, 1H), 7.34 (d, *J* = 8.1 Hz, 1H), 7.42 (d, *J* = 15.9 Hz, 1H), 7.49 (d, *J* = 8.4 Hz, 2H), 7.64 (d, *J* = 7.8 Hz, 1H), 7.85 (d, *J* = 8.7 Hz, 2H), 8.38 (d, *J* = 8.1 Hz, 1H), 8.98 (s, 1H), 10.66 (s, 1H), 10.82 (d, *J* = 1.5 Hz, 1H). HRMS (AP-ESI) *m/z* calcd for C<sub>28</sub>H<sub>27</sub>N<sub>3</sub>O<sub>5</sub> [M + H]<sup>+</sup> 486.2023, found 486.2023. Retention time: 10.1 min, eluted with 47% acetonitrile/53% water (containing 0.4% formic acid).

(*S,E*)-*tert*-Butyl(1-(4-(3-(hydroxyamino)-3-oxoprop-1-en-1-yl)phenoxy)-3-(1-methyl-1*H*-indol-3-yl)propan-2-yl)carbamate (**14**). Pale yellow solid, 33% yield. Mp: 146–148 °C. <sup>1</sup>H NMR (300 MHz, DMSO-*d*<sub>6</sub>) δ 1.36 (s, 9H), 2.83–2.99 (m, 2H), 3.72 (s, 3H), 3.93–4.04 (m, 3H), 6.33 (dd, *J* = 4.5 Hz, *J* = 15.9 Hz, 1H), 6.95 (d, *J* = 8.4 Hz, 2H), 6.97–7.02 (m, 2H), 7.10–7.15 (m, 2H), 7.36–7.42 (m, 2H), 7.49 (d, *J* = 8.4 Hz, 2H), 7.58 (d, *J* = 7.8 Hz, 1H), 8.97 (s, 1H), 10.66 (s, 1H). HRMS (AP-ESI) *m/z* calcd for C<sub>26</sub>H<sub>31</sub>N<sub>3</sub>O<sub>5</sub> [M + H]<sup>+</sup> 466.2336, found 466.2332. Retention time: 13.8 min, eluted with 47% acetonitrile/53% water (containing 0.4% formic acid).

(*S,E*)-*tert*-Butylbenzyl(1-(4-(3-(hydroxyamino)-3-oxoprop-1-en-1-yl)phenoxy)-3-(1*H*-indol-3-yl)propan-2-yl)carbamate (**20a**). A pale yellow solid, 90% yield. <sup>1</sup>H NMR (300 MHz, DMSO-*d*<sub>6</sub>) δ 1.15–1.25 (m, 9H), 2.90–3.06 (m, 2H), 3.97–4.06 (m, 2H), 4.31–4.40 (m, 2H), 4.56 (s, 1H), 6.31 (d, *J* = 15.6 Hz, 1H), 6.76–6.79 (m, 2H), 6.98 (t, *J* = 7.2 Hz, 1H), 7.01–7.07 (m, 2H), 7.09–7.25 (m, 5H), 7.32–7.43 (m, 5H), 8.96 (s, 1H), 10.64 (s, 1H), 10.84 (s, 1H). ESI-MS *m/z*: 541.4 [M + H]<sup>+</sup>.

(*S,E*)-*tert*-Butyl 4-Chlorobenzyl(1-(4-(3-(hydroxyamino)-3-oxoprop-1-en-1-yl)phenoxy)-3-(1*H*-indol-3-yl)propan-2-yl)carbamate (**20b**). A pale yellow oil, 80% yield.

(*S,E*)-*tert*-Butyl 4-Fluorobenzyl(1-(4-(3-(hydroxyamino)-3-oxoprop-1-en-1-yl)phenoxy)-3-(1*H*-indol-3-yl)propan-2-yl)carbamate (**20c**). A pale yellow oil, 85% yield.

(*S,E*)-*N*-(1-(3-(3-(Hydroxyamino)-3-oxoprop-1-en-1-yl)phenoxy)-3-(1*H*-indol-3-yl)propan-2-yl)benzamide (**27a**). A pale yellow powder, 30% yield. Mp: 104–106 °C. <sup>1</sup>H NMR (300 MHz, DMSO-*d*<sub>6</sub>) δ 3.15 (d, *J* = 8.4 Hz, 2H), 4.06–4.11 (m, 1H), 4.16–4.22 (m, 1H), 4.54–4.64 (m, 1H), 6.48 (d, *J* = 15.6 Hz, 1H), 6.94–6.99 (m, 2H), 7.08 (t, *J* = 7.6 Hz, 1H), 7.12–7.14 (m, 2H), 7.19 (d, *J* = 2.4 Hz, 1H), 7.30 (d, *J* = 8.1 Hz, 1H), 7.34 (d, *J* = 7.8 Hz, 1H), 7.38 (d, *J* = 15.9 Hz, 1H), 7.42–7.54 (m, 3H), 7.65 (d, *J* = 7.8 Hz, 1H), 7.82–7.85 (m, 2H), 8.52 (d, *J* = 8.1 Hz, 1H), 9.05 (s, 1H), 10.71 (s, 1H), 10.82 (d, *J* = 1.5 Hz, 1H). HRMS (AP-ESI) *m/z* calcd for C<sub>27</sub>H<sub>25</sub>N<sub>3</sub>O<sub>4</sub> [M + H]<sup>+</sup> 456.1918, found 456.1919. Retention time: 11.5 min, eluted with 46% acetonitrile/54% water (containing 0.4% formic acid).

(*S,E*)-4-Fluoro-*N*-(1-(3-(3-(hydroxyamino)-3-oxoprop-1-en-1-yl)phenoxy)-3-(1*H*-indol-3-yl)propan-2-yl)benzamide (**27b**). A pale yellow powder, 28% yield. Mp: 96–98 °C. <sup>1</sup>H NMR (300 MHz, DMSO-*d*<sub>6</sub>) δ 3.05–3.19 (m, 2H), 4.05–4.11 (m, 1H), 4.13–4.20 (m, 1H), 4.52–4.61 (m, 1H), 6.48 (d, *J* = 15.6 Hz, 1H), 6.94–6.98 (m, 2H), 7.08 (t, *J* = 7.2 Hz, 1H), 7.11–7.18 (m, 3H), 7.26–7.34 (m, 4H), 7.42 (d, *J* = 15.9 Hz, 1H), 7.64 (d, *J* = 7.5 Hz, 1H), 7.89–7.94 (m, 2H), 8.54 (d, *J* = 7.8 Hz, 1H), 9.04 (s, 1H), 10.70 (s, 1H), 10.80 (s, 1H). HRMS (AP-ESI) *m/z* calcd for C<sub>27</sub>H<sub>24</sub>FN<sub>3</sub>O<sub>4</sub> [M + H]<sup>+</sup> 474.1824, found 474.1825.

(*S,E*)-4-Chloro-*N*-(1-(3-(3-(hydroxyamino)-3-oxoprop-1-en-1-yl)phenoxy)-3-(1*H*-indol-3-yl)propan-2-yl)benzamide (**27c**). A pale yellow powder, 33% yield. Mp: 126–127 °C. <sup>1</sup>H NMR (300 MHz, DMSO-*d*<sub>6</sub>) δ 3.09–3.12 (m, 2H), 4.06–4.20 (m, 2H), 4.54–4.61 (m, 1H), 6.48 (d, *J* = 15.9 Hz, 1H), 6.94–6.99 (m, 2H), 7.08 (t, *J* = 7.4 Hz, 1H), 7.12–7.14 (m, 2H), 7.18 (d, *J* = 2.1 Hz, 1H), 7.27–7.34 (m, 2H), 7.42 (d, *J* = 15.6 Hz, 1H), 7.55 (d, *J* = 8.7 Hz, 2H), 7.64 (d, *J* = 7.5 Hz, 1H), 7.88 (d, *J* = 8.7 Hz, 2H), 8.62 (d, *J* = 7.8 Hz, 1H), 9.05 (s, 1H), 10.71 (s, 1H), 10.82 (d, *J* = 1.5 Hz, 1H). HRMS (AP-ESI) *m/z* calcd for C<sub>27</sub>H<sub>24</sub>ClN<sub>3</sub>O<sub>4</sub> [M + H]<sup>+</sup> 456.1918, found 456.1919. Retention time: 17.2 min, eluted with 40% acetonitrile/60% water (containing 0.4% formic acid).

**General Procedure for the Preparation of 21a–21c.** (*S,E*)-*tert*-Butylbenzyl(1-(4-(3-(hydroxyamino)-3-oxoprop-1-en-1-yl)phenoxy)-3-(1*H*-indol-3-yl)propan-2-yl)carbamate (**21a**). This method was the same as the general procedure for the preparation of **8** and **25**.

A pale yellow oil, 65% yield. Mp: 136–138 °C. <sup>1</sup>H NMR (300 MHz, DMSO-*d*<sub>6</sub>) δ 3.17–3.27 (m, 1H), 3.41–3.47 (m, 1H), 3.67 (s, 1H), 4.12–4.17 (m, 1H), 4.25–4.27 (m, 1H), 4.36 (s, 2H), 6.38 (d, *J* = 15.6 Hz, 1H), 6.91–6.99 (m, 3H), 7.10 (t, *J* = 7.2 Hz, 1H), 7.22 (d, *J* = 2.4 Hz, 1H), 7.37 (d, *J* = 7.8 Hz, 2H), 7.42–7.50 (m, 6H), 7.64–7.68 (m, 2H), 9.72 (s, 1H), 9.92 (s, 1H), 10.31 (s, 1H), 11.05 (d, *J* = 1.8 Hz, 1H). HRMS (AP-ESI) *m/z* calcd for C<sub>27</sub>H<sub>27</sub>N<sub>3</sub>O<sub>3</sub> [M + H]<sup>+</sup> 442.2125, found 442.2125. Retention time: 12.5 min.

(*S,E*)-*tert*-Butyl 4-Fluorobenzyl(1-(4-(3-(hydroxyamino)-3-oxoprop-1-en-1-yl)phenoxy)-3-(1*H*-indol-3-yl)propan-2-yl)carbamate (**21b**). A pale yellow oil, 68% yield. Mp: 138–140 °C. <sup>1</sup>H NMR (300 MHz, DMSO-*d*<sub>6</sub>) δ 3.17–3.26 (m, 1H), 3.41–3.48 (m, 1H), 3.70 (s, 1H), 4.12–4.17 (m, 1H), 4.25–4.28 (m, 1H), 4.36 (s, 2H), 6.39 (d, *J* = 15.9 Hz, 1H), 6.92–6.99 (m, 3H), 7.10 (t, *J* = 6.9 Hz, 1H), 7.23 (d, *J* = 2.1 Hz, 1H), 7.29 (d, *J* = 8.7 Hz, 2H), 7.35–7.42 (m, 2H), 7.48–7.53 (m, 3H), 7.69–7.74 (m, 2H), 9.74 (s, 1H), 9.94 (s, 1H), 11.05 (d, *J* = 1.8 Hz, 1H). HRMS (AP-ESI) *m/z* calcd for C<sub>27</sub>H<sub>26</sub>FN<sub>3</sub>O<sub>3</sub> [M + H]<sup>+</sup> 460.2031, found 460.2033. Retention time: 14.2 min.

(*S,E*)-*tert*-Butyl 4-Chlorobenzyl(1-(4-(3-(hydroxyamino)-3-oxoprop-1-en-1-yl)phenoxy)-3-(1*H*-indol-3-yl)propan-2-yl)carbamate (**21c**). A pale yellow oil, 60% yield. Mp: 136–138 °C. <sup>1</sup>H NMR (300 MHz, DMSO-*d*<sub>6</sub>) δ 3.17–3.26 (m, 1H), 3.41–3.47 (m, 2H), 4.11–4.16 (m, 1H), 4.24–4.27 (m, 1H), 4.37 (s, 2H), 6.38 (d, *J* = 15.9 Hz, 1H), 6.92–6.99 (m, 3H), 7.11 (t, *J* = 7.2 Hz, 1H), 7.23 (d, *J* = 2.1 Hz, 1H), 7.37 (d, *J* = 8.1 Hz, 1H), 7.42 (d, *J* = 15.6 Hz, 1H), 7.48–7.53 (m, 5H), 7.70 (d, *J* = 8.4 Hz, 2H), 9.75 (s, 1H), 9.69 (s, 1H), 10.30 (s, 1H), 11.05 (d, *J* = 1.8 Hz, 1H). HRMS (AP-ESI) *m/z* calcd for C<sub>27</sub>H<sub>26</sub>ClN<sub>3</sub>O<sub>3</sub> [M + H]<sup>+</sup> 476.1735, found 476.1735. Retention time: 21.3 min.

**In Vitro HDACs Inhibition Fluorescence Assay.** In vitro HDACs inhibition assays were conducted as previously described.<sup>22</sup> In brief, 10 μL of enzyme solution (HeLa nuclear extract, HDAC1, HDAC2, HDAC3, or HDAC6) was mixed with various concentrations of tested compound (50 μL). The mixture was incubated at 37 °C for 5 min, then fluorogenic substrate Boc-Lys(acetyl)-AMC (40 μL) was added. After incubation at 37 °C for 30 min, the mixture was stopped by the addition of 100 μL of developer containing trypsin and TSA. Twenty minutes later, fluorescence intensity was measured using a microplate reader at excitation and emission wavelengths of 390 and 460 nm, respectively. The inhibition ratios were calculated from the fluorescence intensity readings of tested wells relative to those of control wells, and the IC<sub>50</sub> values were calculated using a regression analysis of the concentration/inhibition data.

**In Vitro Antiproliferative Assay.** All cell lines were maintained in RPMI1640 medium containing 10% FBS at 37 °C in a 5% CO<sub>2</sub> humidified incubator. Cell proliferation assay was determined by the MTT method. Briefly, cells were passaged the day before dosing into a 96-well cell plate, allowed to grow for 12 h and then treated with different concentrations of compound sample for 48 h. A 0.5% MTT solution was added to each well. After incubation for another 4 h, formazan formed from MTT was extracted by adding 150 μL of DMSO rocking for 15 min. Absorbance was then determined using an ELISA reader at 570 nm.

**Western Blot Analysis.** Briefly, U937 cells with different treatment were collected and lysed with lysis buffer (20 mM Tris-HCl [pH 7.5], 1% NP-40, 1 mM sodium vanadate, 1 mM EDTA, 1 mM EGTA, 50 mM NaF, and 1 mM phenylmethyl sulfonylfluoride [PMSF]) for 30 min, then centrifuged for 15 min at 14 000 rpm at 4 °C, and the supernatant was the whole-cell extracts. Total protein extracts (30 μg per lane) were separated by 12% SDS polyacrylamide gel electrophoresis and transferred onto PVDF membranes (Cat. IPVH00010, Millipore). Membrane was blocked with 5% S36 milk in TBS-T (10 mM Tris [pH 7.4], 150 mM NaCl, and 0.1% Tween 20) for 1 h at room temperature, then incubated with a 1:1000 or 1:2000 dilution of primary antibody overnight at 4 °C. Then the membrane was washed three times and incubated at 1:2000 dilution of antimouse or anti-rabbit goat-HRP-conjugated secondary antibodies for 2 h at room temperature. Finally the membrane was washed another three times and developed by enhanced chemiluminescence (ECL, Cat. WBKLS0050, Millipore).

**Apoptosis Assay.** U937 cells (1.5 × 10<sup>5</sup>) were treated with different concentrations of **11r**, **11w**, or SAHA for 12 or 24 h. Cells were harvested following incubation, washed twice in cold PBS, centrifuged, and resuspended in 1× annexin-binding buffer. Cells were diluted in 1× annexin-binding buffer to 1 × 10<sup>6</sup> cells/mL, preparing a sufficient volume to have 100 μL per assay. Five microliters of Alexa Fluor 488 annexin V and 1 μL of 100 μg/mL PI were added to each 100 μL of cell suspension. Cells were incubated at room temperature for 15 min. After the incubation period, 150 μL of 1× annexin-binding buffer was added, mixed gently, and kept on ice. The stained cells were analyzed by flow cytometry, measuring the fluorescence emission at 530 and 575 nm (or equivalent) using 488 nm excitation. Alexa Fluor 488 annexin V/Dead Cell Apoptosis Kit with Alexa Fluor 488 annexin V and PI for Flow Cytometry was used for this assay (Invitrogen).

**Stability of Representative Compound in Artificial Gastric Juice, Artificial Intestinal Juice, Rat Liver Homogenate, and Human Plasma.** Preparation of artificial gastric juice: 160 mL of water and 2 g of pepsin were added to 3.28 mL of diluted hydrochloric acid. After mixing, the mixture was diluted to 200 mL with water. Preparation of artificial intestinal juice: 1.36 g of sodium dihydrogen phosphate was dissolved in 100 mL of water, and the pH was adjusted to 6.8 using 0.4% NaOH. Then 2 g of pancreatin was added, and the mixture was diluted to 200 mL with water. Preparation of rat liver homogenate: Wistar rats (Experimental Animal Center, Shandong University, female, 200 ± 20 g) were sacrificed after fasting 12 h. Liver was homogenized in quadruple phosphate buffer (pH 7.4) and centrifuged (4000 rpm), 10 min. The liver homogenate was stored at –20 °C. Human plasma was obtained from Institution of Clinical Pharmacology, Qilu Hospital. Artificial gastric juice, artificial intestinal juice, rat liver homogenate, and human plasma were preincubated at 37 °C prior to the addition of 50 μL of stock solution of mutual prodrugs (1 mg/mL in CH<sub>3</sub>OH). Sample aliquots were taken for processing and analysis after 24 h incubation at 37 °C. All of the samples underwent extraction using 600 μL acetonitrile and were filtered (0.22 μm) after shocking 30 s and centrifugation at 12 000 rpm, 10 min. Chromatographic analysis was achieved by HPLC method on an Agilent 1100 HPLC instrument using a ODS HYPERSIL column (5 μm, 4.6 mm × 100 mm) according the following method: compound was eluted with 42% acetonitrile/58% water (containing 0.4% formic acid) over 20 min, with detection at 290 nm and a flow rate of 1 mL/min. The temperature of the column was 25 °C, and the quantity of injection was 20 μL.

**In Vivo Antitumor Assay against U937 Xenograft.** For in vivo antitumor efficacy research, 1 × 10<sup>7</sup> human histiocytic lymphoma cells (U937) were inoculated subcutaneously in the right flank of male athymic nude mice (5–6 weeks old, SLAC LABORATORY ANIMAL, Shanghai). Ten days after injection, tumors were palpable, and mice were randomized into treatment and control groups (5 mice per group). The treatment groups received compound **11r** (100 mg/kg/d) or SAHA (100 mg/kg/d) by oral administration, and the blank control group received equal volume of PBS solution containing 40% DMSO. During treatment, subcutaneous tumors were measured with a vernier caliper every three days, and body weight was monitored regularly.



After treatment, mice were sacrificed and dissected to weigh the tumor tissues and to examine the internal organ injury. Tumor growth inhibition (TGI) and relative increment ratio (T/C) were used as the evaluation indicators to reveal the antitumor effects in tumor weight and tumor volume, respectively. Data were analyzed by Student's two-tailed *t* test. A *P* level < 0.05 was considered statistically significant.

$$\text{TGI} = \left( \frac{\text{the mean tumor weight of control group} - \text{the mean tumor weight of treated group}}{\text{the mean tumor weight of control group}} \right)$$

Tumor volumes (*V*) were estimated using the equation ( $V = ab^2/2$ , where *a* and *b* stand for the longest and shortest diameter, respectively). T/C was calculated according to the following formula:

$$\text{T/C} = \frac{\text{the mean RTV of treated group}}{\text{the mean RTV of control group}}$$

where RTV is the relative tumor volume =  $V_t/V_0$  ( $V_t$ , the tumor volume measured at the end of treatment;  $V_0$ , the tumor volume measured at the beginning of treatment).

**Molecular Docking Studies.** Compounds were docked into the active site of HDAC3 (PDB code 4A69) using Tripos SYBYL 8.0. Before the docking process, the protein structure was treated by deleting water molecules, adding hydrogen atoms, fixing atom types, and assigning AMBER7 FF99 charges. A 100-step minimization process was performed to further optimize the protein structure. The molecular structures were generated with the Sybyl/Sketch module and optimized using Powell's method with the Tripos force field with convergence criterion set at 0.05 kcal/(Å mol) and assigned charges with the Gasteiger–Hückel method. Molecular docking was carried out via the Sybyl/FlexX module. Other docking parameters were kept to the default values.

## ■ ASSOCIATED CONTENT

### ■ Supporting Information

<sup>1</sup>H NMR spectral information of the key intermediates **6**, **7**, and **8** and representative target compounds **10a**, **11k**, **11e**, **11p**, **11r**, **11w**, **11y**, and **27c**. HPLC analysis chromatograms of representative target compounds **10a**, **11k**, **11e**, **11p**, **11r**, **11w**, **11y**, and **27c**. This material is available free of charge via the Internet at <http://pubs.acs.org>.

## ■ AUTHOR INFORMATION

### Corresponding Authors

\* (W.X.) Phone: 86-531-88382264. Fax: 86-531-88382264. E-mail: [wenfuxu@gmail.com](mailto:wenfuxu@gmail.com).

\* (Y.Z.) E-mail: [zhangyingjie@sdu.edu.cn](mailto:zhangyingjie@sdu.edu.cn)

### Author Contributions

The manuscript was written through contributions of all authors. All authors have given approval to the final version of the manuscript.

### Notes

The authors declare no competing financial interest.

## ■ ACKNOWLEDGMENTS

This work was supported by National Scientific and Technological Major Project of Ministry of Science and Technology of China (Grant no. 2011ZX09401-015), National Natural Science Foundation of China (Grant no. 21302111 and 21172134), China Postdoctoral Science Foundation funded project (Grant no. 2013M540558), Postdoctoral Innovation Project Foundation of Shandong Province (Grant No.201303090), Independent Innovation Foundation of Shandong University, IIFSDU (Grant no. 2013GN013),

National Cancer Institute of the National Institutes of Health (Award no. R01CA163452) and National High-tech R&D Program of China, 863 Program (Grant No.2014AA020523).

## ■ ABBREVIATIONS USED

HDAC, histone deacetylase; HDACi, histone deacetylase inhibitors; SAR, structure–activity relationships; SAHA, suberoylanilide hydroxamic acid; ZBG, zinc-binding group; Boc, tertbutoxycarbonyl

## ■ REFERENCES

- (1) Herman, J. G.; Baylin, S. B. Gene silencing in cancer in association with promoter hypermethylation. *N. Engl. J. Med.* **2003**, *349*, 2042–2054.
- (2) Zhang, Y.; Fang, H.; Jiao, J.; Xu, W. The structure and function of histone deacetylases: the target for anti-cancer therapy. *Curr. Med. Chem.* **2008**, *15*, 2840–2849.
- (3) Kristensen, L. S.; Nielsen, H. M.; Hansen, L. L. Epigenetics and cancer treatment. *Eur. J. Pharmacol.* **2009**, *625*, 131–142.
- (4) Gregoret, I.; Lee, Y.-M.; Goodson, H. V. Molecular evolution of the histone deacetylase family: functional implications of phylogenetic analysis. *J. Mol. Biol.* **2004**, *338*, 17–31.
- (5) Stünkel, W.; Campbell, R. M. Sirtuin 1 (SIRT1) the misunderstood HDAC. *J. Biomol. Screening* **2011**, *16*, 1153–1169.
- (6) Lagger, G.; O'Carroll, D.; Rembold, M.; Khier, H.; Tischler, J.; Weitzer, G.; Schuettengruber, B.; Hauser, C.; Brunmeir, R.; Jenuwein, T. Essential function of histone deacetylase 1 in proliferation control and CDK inhibitor repression. *EMBO J.* **2002**, *21*, 2672–2681.
- (7) Simboeck, E.; Di Croce, L. HDAC1, a novel marker for benign teratomas. *EMBO J.* **2010**, *29*, 3893–3895.
- (8) Pilarsky, C.; Wenzig, M.; Specht, T.; Saeger, H. D.; Grutzmann, R. Identification and validation of commonly overexpressed genes in solid tumors by comparison of microarray data. *Neoplasia* **2004**, *6*, 744–750.
- (9) Karagianni, P.; Wong, J. HDAC3: taking the SMRT-N-CoR ect road to repression. *Oncogene* **2007**, *26*, 5439–5449.
- (10) (a) Wilson, A. J.; Byun, D.-S.; Popova, N.; Murray, L. B.; L'Italien, K.; Sowa, Y.; Arango, D.; Velcich, A.; Augenlicht, L. H.; Mariadason, J. M. Histone deacetylase 3 (HDAC3) and other class I HDACs regulate colon cell maturation and p21 expression and are deregulated in human colon cancer. *J. Biol. Chem.* **2006**, *281*, 13548–13558. (b) Godman, C. A.; Joshi, R.; Tierney, B. R.; Greenspan, E.; Rasmussen, T. P.; Wang, H.-W.; Shin, D.-G.; Rosenberg, D. W.; Giardina, C. HDAC3 impacts multiple oncogenic pathways in colon cancer cells with effects on Wnt and vitamin D signaling. *Cancer Biol. Ther.* **2008**, *7*, 1570–1580.
- (11) Glaser, K. B.; Li, J.; Staver, M. J.; Wei, R.-Q.; Albert, D. H.; Davidsen, S. K. Role of class I and class II histone deacetylases in carcinoma cells using siRNA. *Biochem. Biophys. Res. Commun.* **2003**, *310*, 529–536.
- (12) Feng, L.; Pan, M.; Sun, J.; Lu, H.; Shen, Q.; Zhang, S.; Jiang, T.; Liu, L.; Jin, W.; Chen, Y. Histone deacetylase 3 inhibits expression of PUMA in gastric cancer cells. *J. Mol. Med.* **2013**, *91*, 49–58.
- (13) Zhu, J.; Wan, H.; Xue, C.; Jiang, T.; Qian, C.; Zhang, Y. Histone deacetylase 3 implicated in the pathogenesis of children glioma by promoting glioma cell proliferation and migration. *Brain Res.* **2013**, *1520*, 15–22.
- (14) Fritzsche, F. R.; Weichert, W.; Röske, A.; Gekeler, V.; Beckers, T.; Stephan, C.; Jung, K.; Scholman, K.; Denkert, C.; Dietel, M. Class I histone deacetylases 1, 2 and 3 are highly expressed in renal cell cancer. *BMC Cancer* **2008**, *8*, 381.
- (15) Yang, Z.; Zhou, L.; Wu, L.-M.; Xie, H.-Y.; Zhang, F.; Zheng, S.-S. Combination of polymorphisms within the HDAC1 and HDAC3 gene predict tumor recurrence in hepatocellular carcinoma patients that have undergone transplant therapy. *Clin. Chem. Lab. Med.* **2010**, *48*, 1785–1791.
- (16) Van Damme, M.; Crompot, E.; Meuleman, N.; Mineur, P.; Bron, D.; Lagneaux, L.; Stamatopoulos, B. HDAC isoenzyme

expression is deregulated in chronic lymphocytic leukemia B-cells and has a complex prognostic significance. *Epigenetics* **2012**, *7*, 1403–1412.

(17) Moffat, D.; Patel, S.; Day, F.; Belfield, A.; Donald, A.; Rowlands, M.; Wibawa, J.; Brotherton, D.; Stimson, L.; Clark, V. *J. Med. Chem.* **2010**, *53*, 8663.

(18) Arts, J.; King, P.; Mariën, A.; Floren, W.; Beliën, A.; Janssen, L.; Pilatte, I.; Roux, B.; Decrane, L.; Gilissen, R. *Clin. Cancer Res.* **2009**, *15*, 6841.

(19) (a) Bergman, J. A.; Woan, K.; Perez-Villarroel, P.; Villagra, A.; Sotomayor, E. M.; Kozikowski, A. P. Selective histone deacetylase 6 inhibitors bearing substituted urea linkers inhibit melanoma cell growth. *J. Med. Chem.* **2012**, *55*, 9891–9899. (b) Gupta, P. K.; Reid, R. C.; Liu, L.; Lucke, A. J.; Broomfield, S. A.; Andrews, M. R.; Sweet, M. J.; Fairlie, D. P. Inhibitors selective for HDAC6 in enzymes and cells. *Bioorg. Med. Chem. Lett.* **2010**, *20*, 7067–7070.

(20) Bürlri, R. W.; Luckhurst, C. A.; Aziz, O.; Matthews, K. L.; Yates, D.; Lyons, K. A.; Beconi, M.; McAllister, G.; Breccia, P.; Stott, A. J. Design, synthesis, and biological evaluation of potent and selective Class IIa histone deacetylase (HDAC) inhibitors as a potential therapy for Huntington's disease. *J. Med. Chem.* **2013**, *56*, 9934–9954.

(21) Shi, B.; Xu, W. The development and potential clinical utility of biomarkers for HDAC inhibitors. *Drug Discovery Ther.* **2013**, *7*, 129–136.

(22) Prince, H. M.; Bishton, M. J.; Harrison, S. J. Clinical studies of histone deacetylase inhibitors. *Clin. Cancer Res.* **2009**, *15*, 3958–3969.

(23) Boumber, Y.; Younes, A.; Garcia-Manero, G. Mocetinostat (MGCD0103): a review of an isotype-specific histone deacetylase inhibitor. *Expert Opin. Invest. Drugs* **2011**, *20*, 823–829.

(24) Moradei, O. M.; Mallais, T. C.; Frechette, S.; Paquin, I.; Tessier, P. E.; Leit, S. M.; Fournel, M.; Bonfils, C.; Trachy-Bourget, M.-C.; Liu, J. Novel aminophenyl benzamide-type histone deacetylase inhibitors with enhanced potency and selectivity. *J. Med. Chem.* **2007**, *50*, 5543–5546.

(25) Methot, J. L.; Chakravarty, P. K.; Chenard, M.; Close, J.; Cruz, J. C.; Dahlberg, W. K.; Fleming, J.; Hamblett, C. L.; Hamill, J. E.; Harrington, P. Exploration of the internal cavity of histone deacetylase (HDAC) with selective HDAC1/HDAC2 inhibitors (SHI-1: 2). *Bioorg. Med. Chem. Lett.* **2008**, *18*, 973–978.

(26) Zhang, Y.; Yang, P.; Chou, C. J.; Liu, C.; Wang, X.; Xu, W. Development of *N*-hydroxycinnamamide-based histone deacetylase inhibitors with an indole-containing cap group. *ACS Med. Chem. Lett.* **2013**, *4*, 235–238.

(27) (a) Hubbert, C.; Guardiola, A.; Shao, R.; Kawaguchi, Y.; Ito, A.; Nixon, A.; Yoshida, M.; Wang, X.-F.; Yao, T.-P. HDAC6 is a microtubule-associated deacetylase. *Nature* **2002**, *417*, 455–458. (b) Zhang, Y.; Li, N.; Caron, C.; Matthias, G.; Hess, D.; Khochbin, S.; Matthias, P. HDAC-6 interacts with and deacetylates tubulin and microtubules in vivo. *EMBO J.* **2003**, *22*, 1168–1179.

(28) Spencer, S. L.; Sorger, P. K. Measuring and modeling apoptosis in single cells. *Cell* **2011**, *144*, 926–939.

(29) Teksin, Z. S.; Seo, P. R.; Polli, J. E. Comparison of drug permeabilities and BCS classification: Three lipid-component PAMPA system method versus Caco-2 monolayers. *AAPS J.* **2010**, *12*, 238–241.